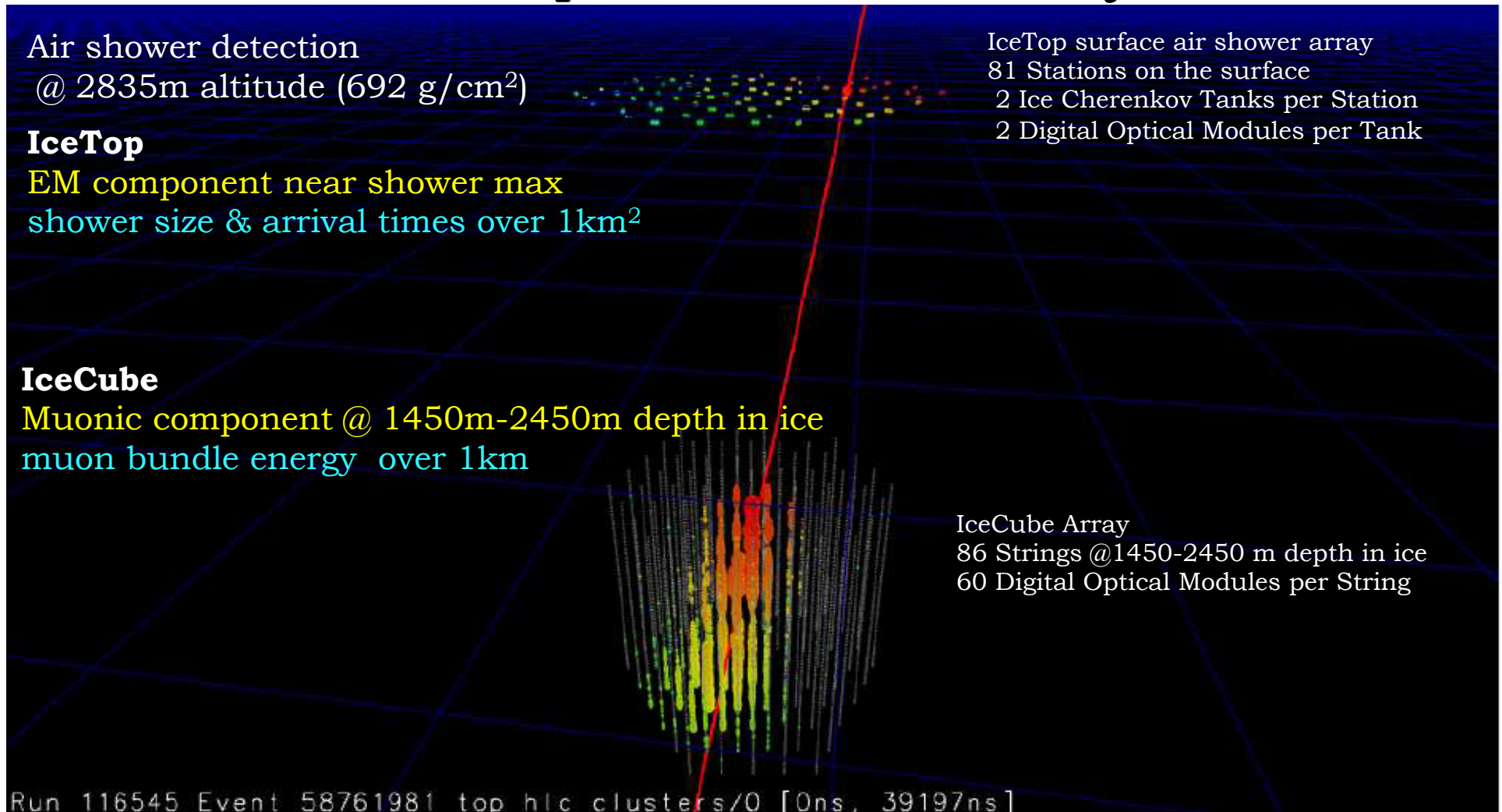


Energy Spectrum & Composition
measured by IceTop/IceCube
&
Global View of Cosmic Ray Data

Serap Tilav
Bartol Research Institute
University of Delaware

SUGAR2015 Jan /21-23/2015 Genève

IceCube Neutrino Telescope & 3D Cosmic Ray Detector

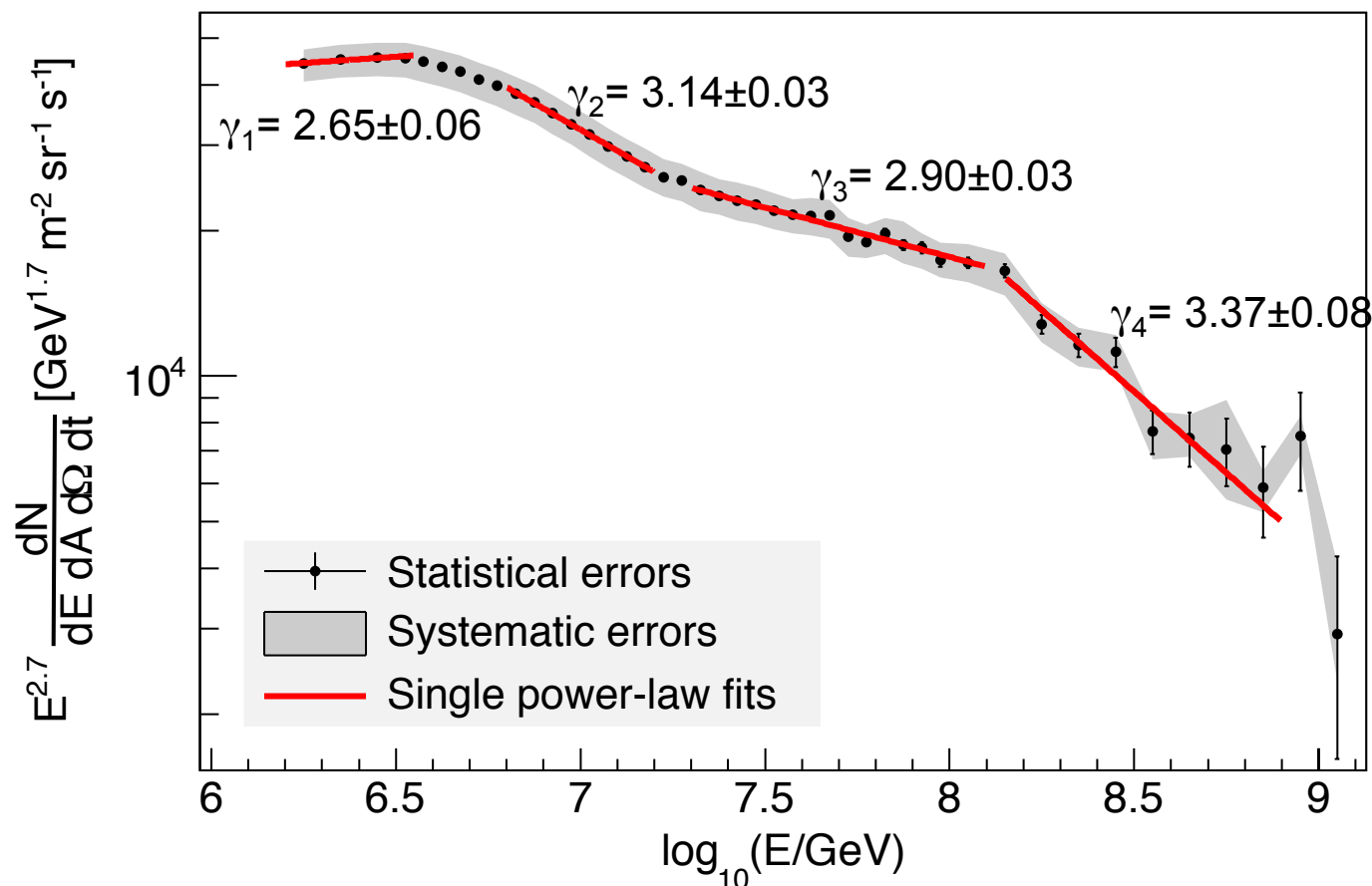


IceTop: Calibration device for IceCube

➔ measure cosmic ray spectrum and composition as input to neutrino calculations

IceTop-73 Analysis

Energy spectrum 1.58 PeV to 1.26 EeV

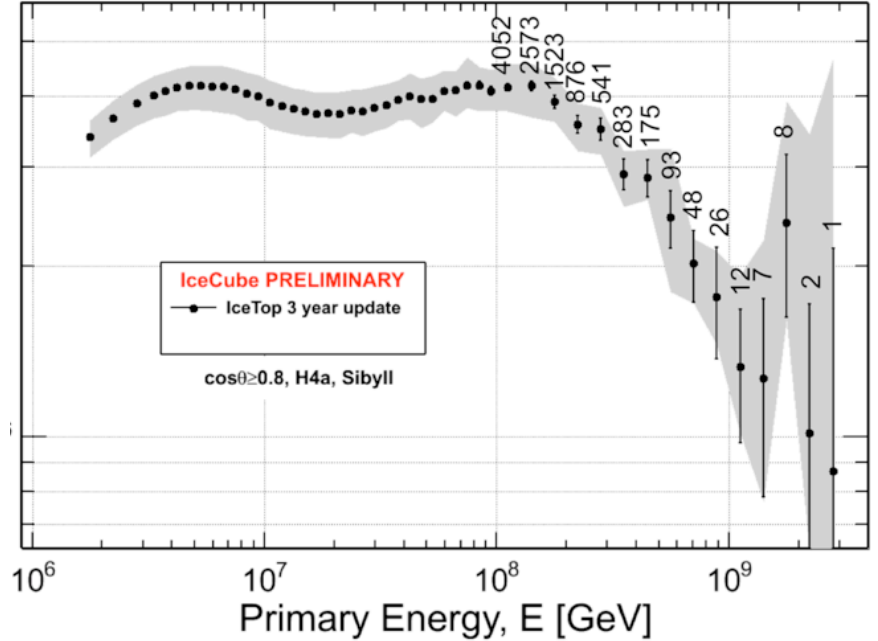
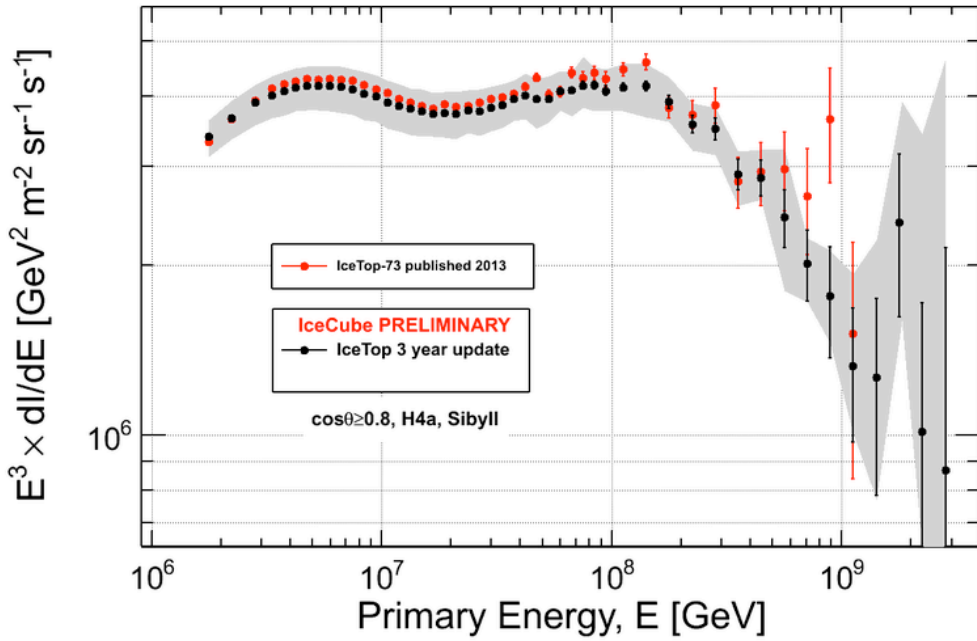


Large scale structure
in spectrum

- Spectrum does not follow a simple power law above the knee up to 1 EeV.
- Spectral hardening at 18 ± 2 PeV (124800 events expected, 139880 observed)
- Spectrum steepens at 130 ± 30 PeV (4213 events expected, 3673 observed)

IceCube, Phys. Rev. D 88, 042004 (2013)

Update: IceTop spectrum with 3 years data

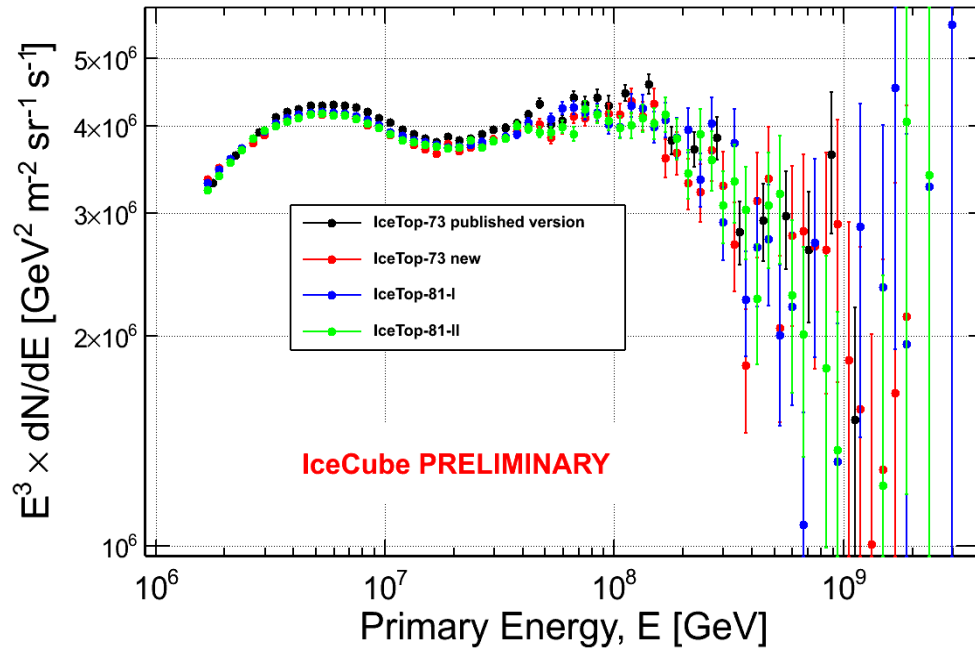


1-2% decrease in the whole energy region with respect to the published spectrum

due to better understanding of snow attenuation

Number of events per bin above 100 PeV

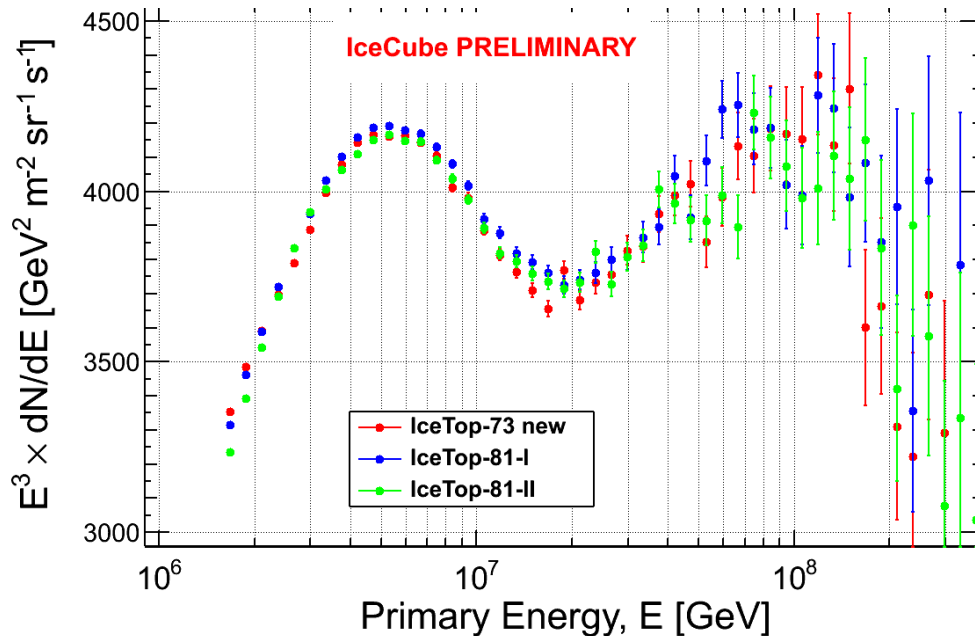
Comparison of yearly spectra



3 individual yearly spectra compared to the published version.

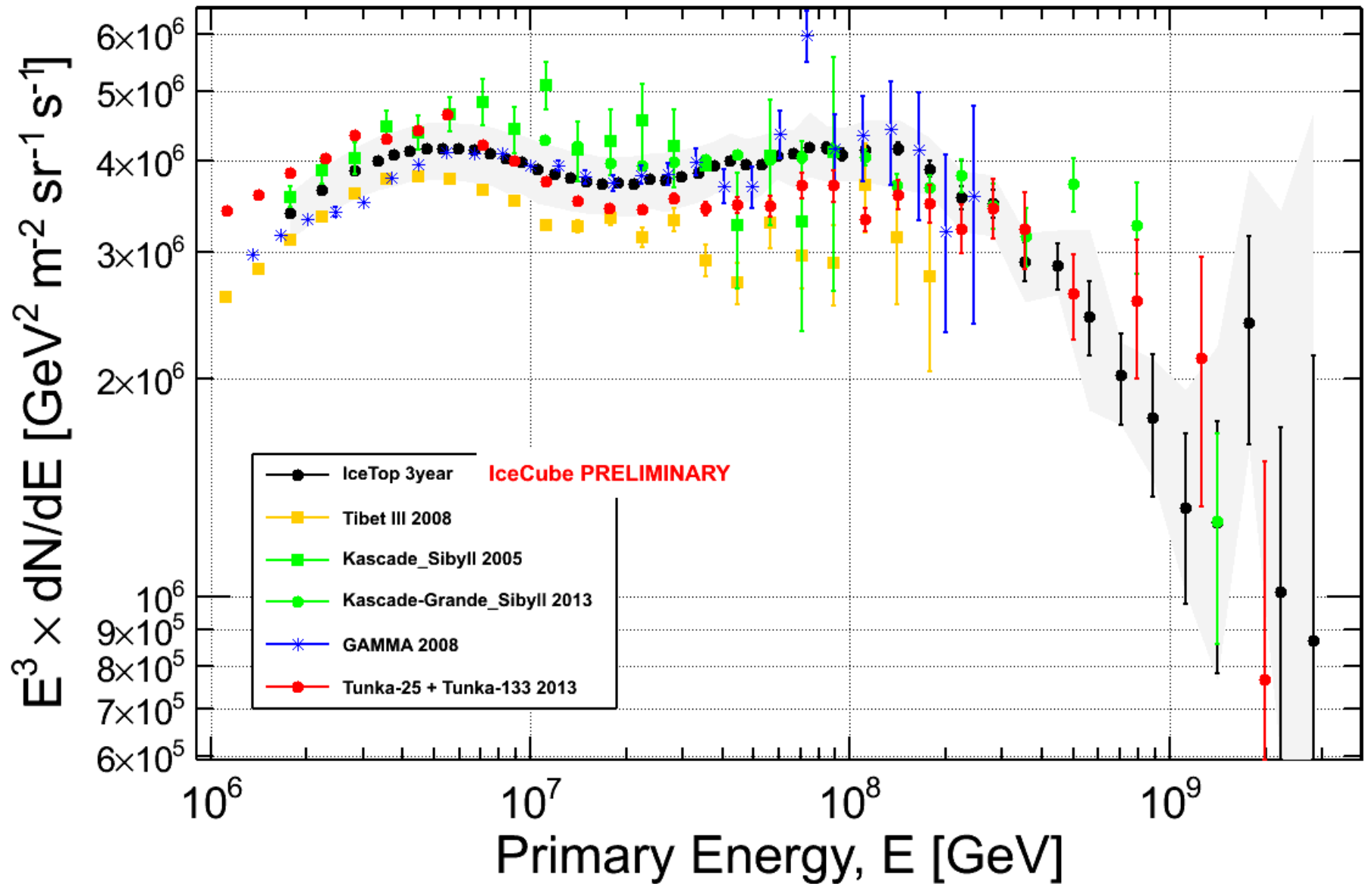
No energy shift is observed between the old and the new spectrum.

The new flux is 1-2% lower than the published one.

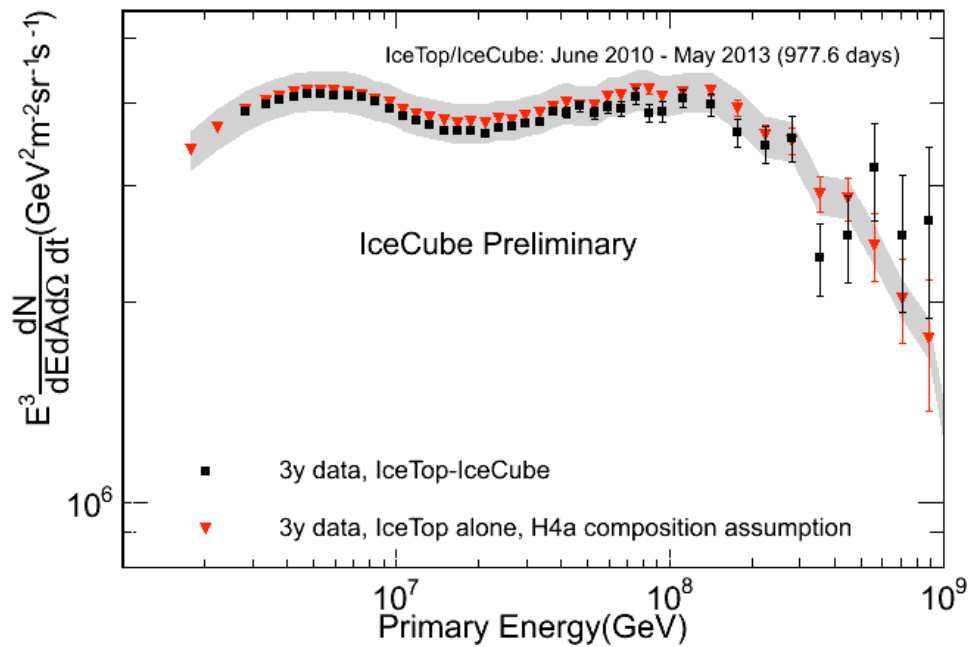


Closer look to their difference

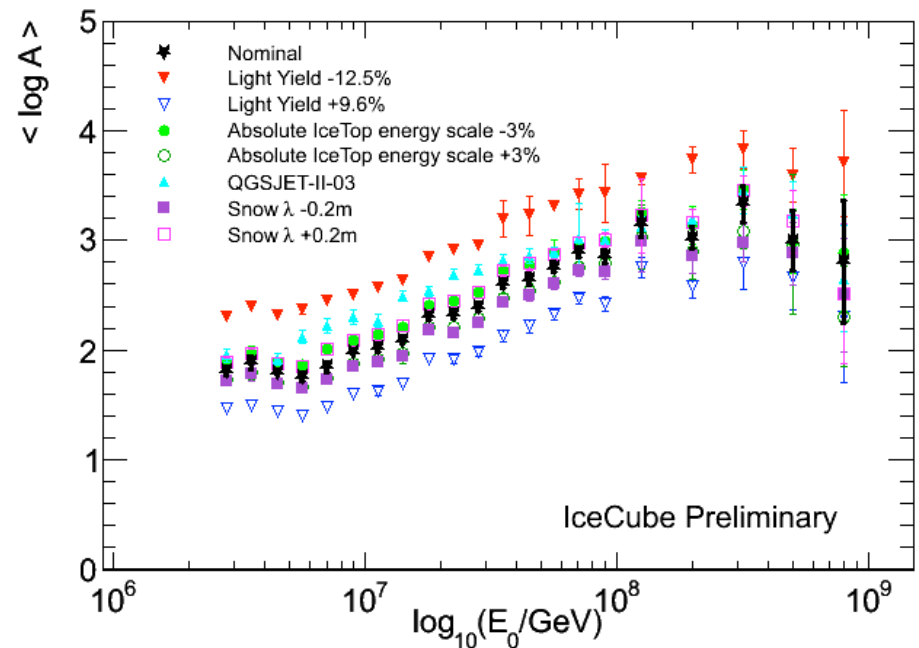
IceTop 3 years spectrum and other experiments



IceTop/IceCube Coincidence Analysis Spectrum & Composition



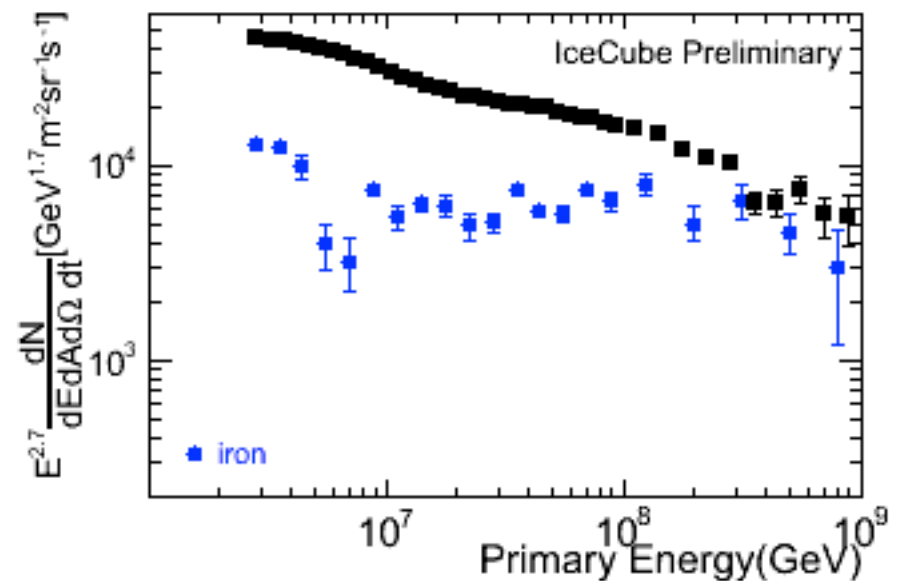
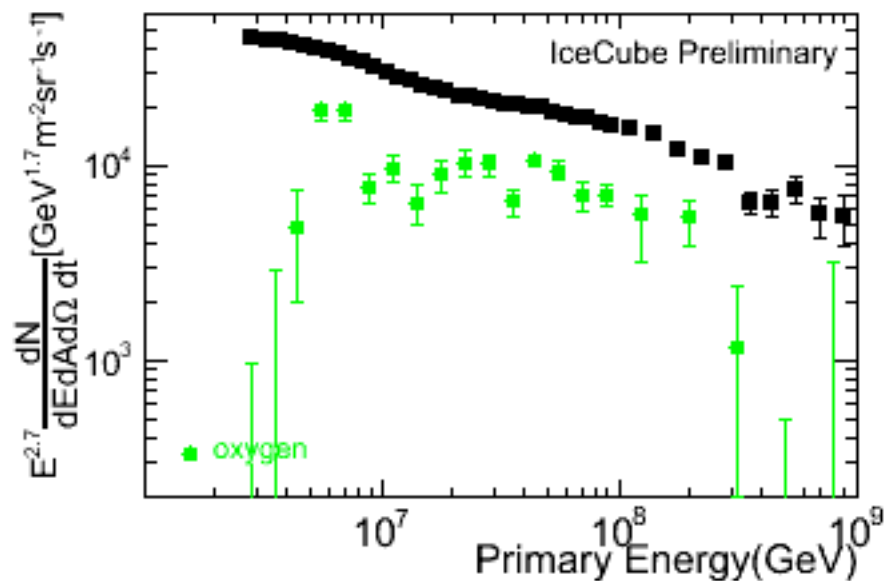
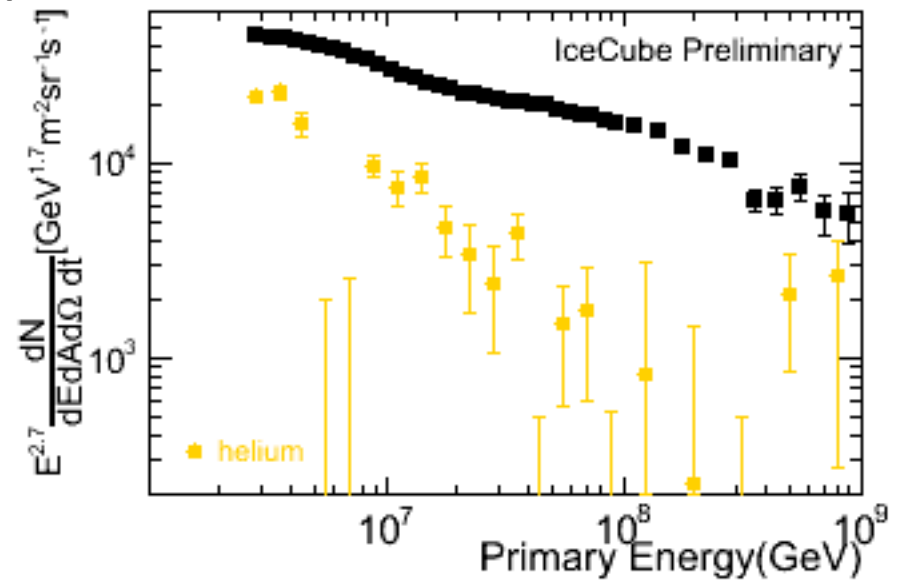
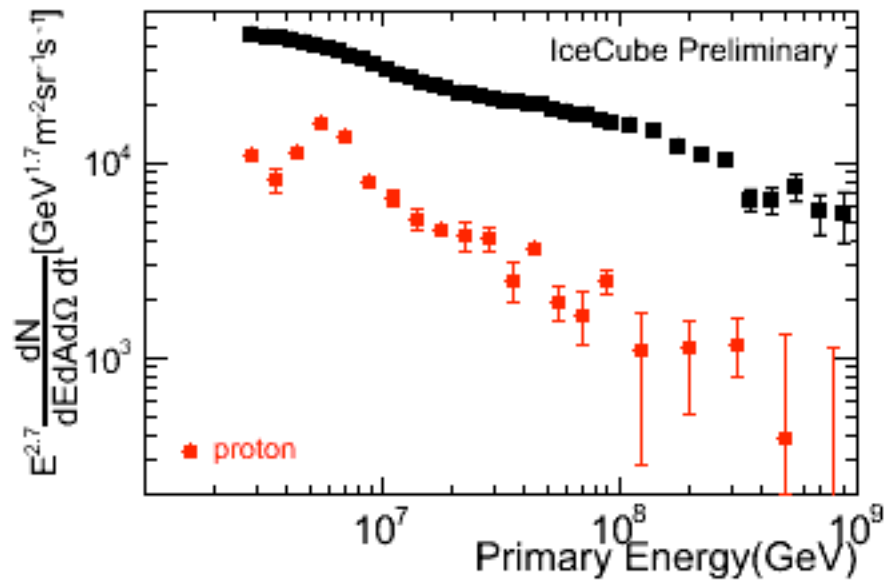
IceTop/IceCube spectrum compared to IceTop spectrum (with its 7% composition uncertainty as error band)



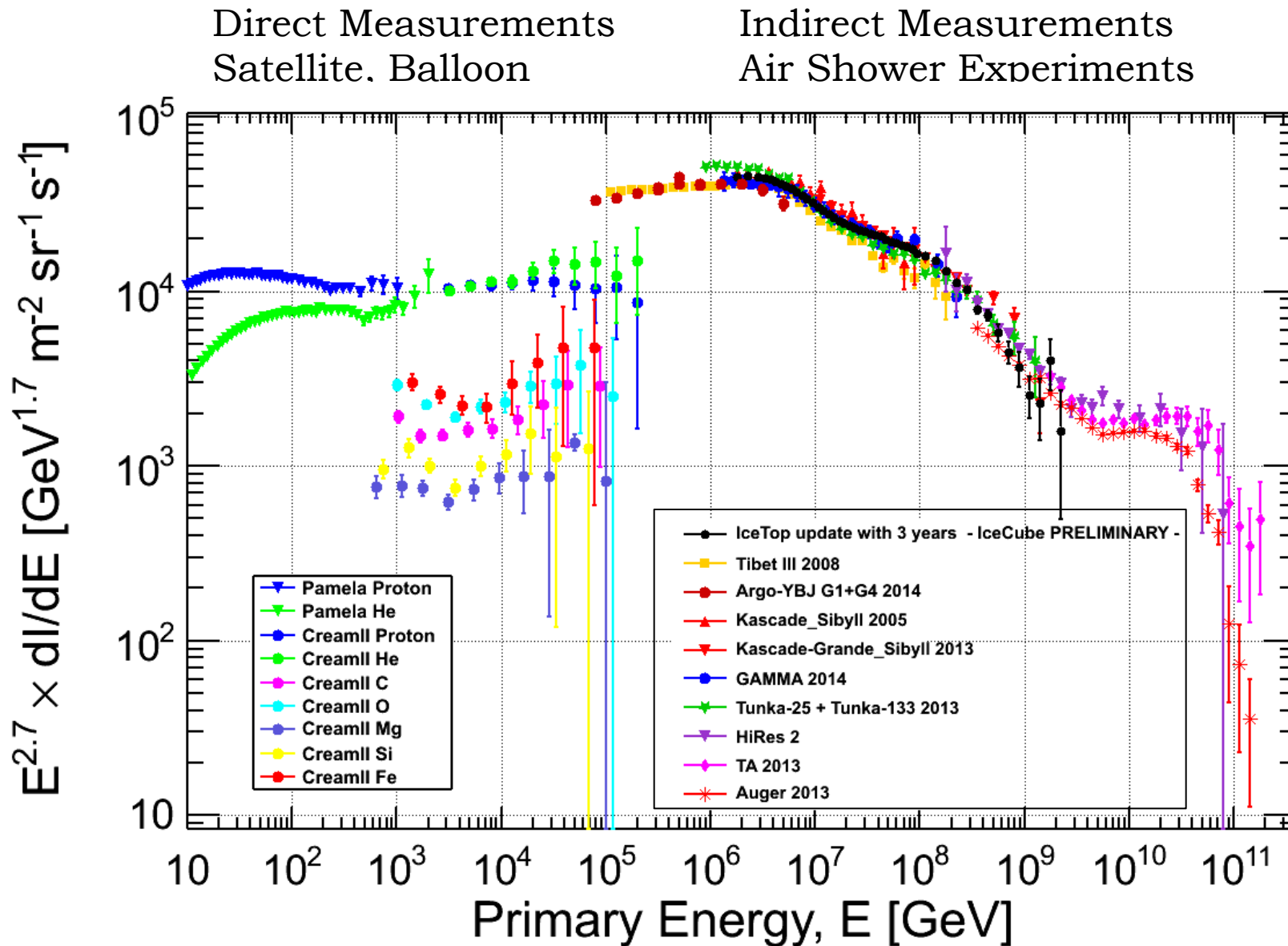
Mean log mass with all systematic uncertainties.

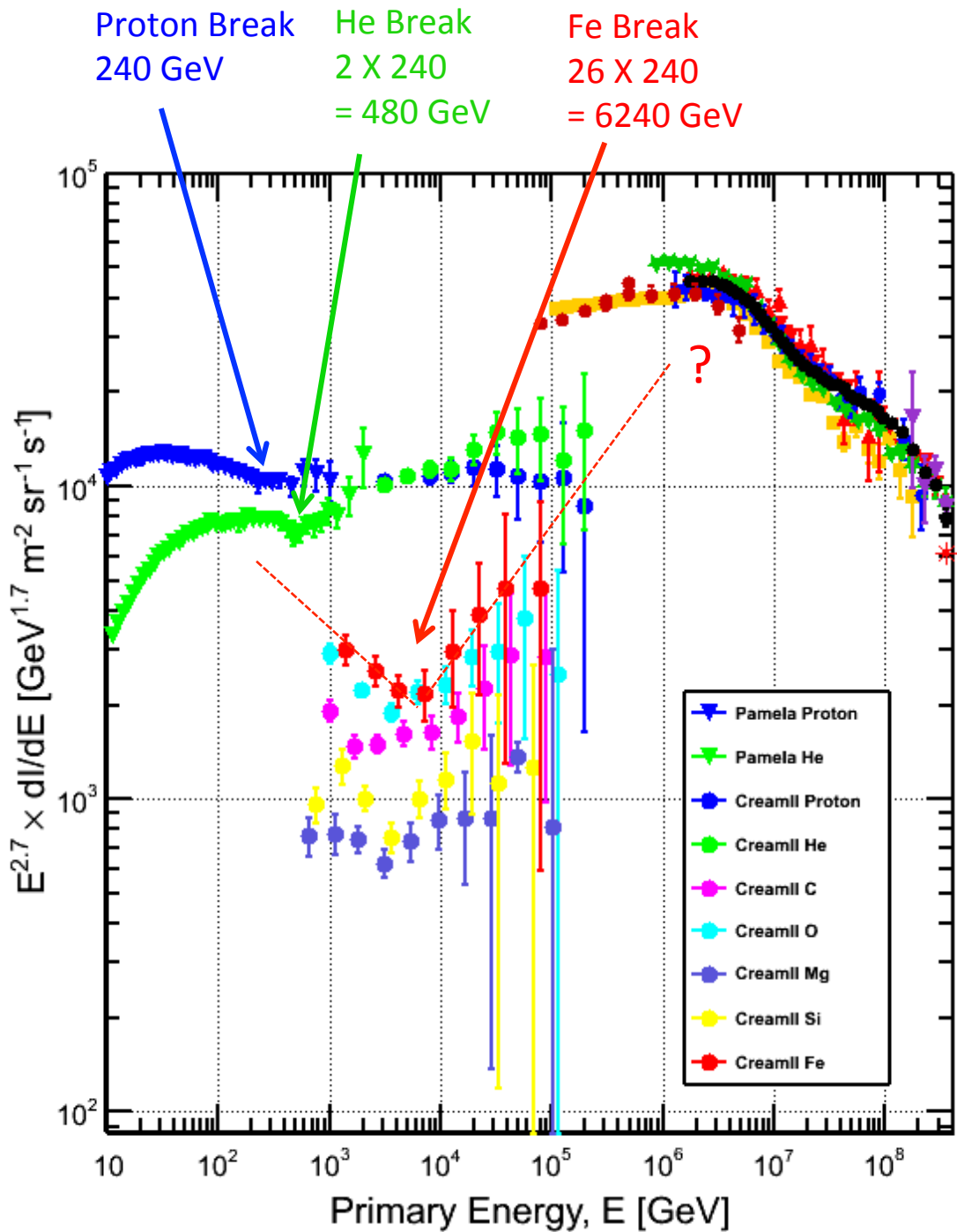
IceTop/IceCube Coincidence Analysis

Elemental Spectra



When looked in detail the CR spectrum is not a simple power law





PAMELA /ATIC/ CREAM
 reveal rigidity dependent
 spectral breaks
 and
 remarkable hardening
 after the breaks

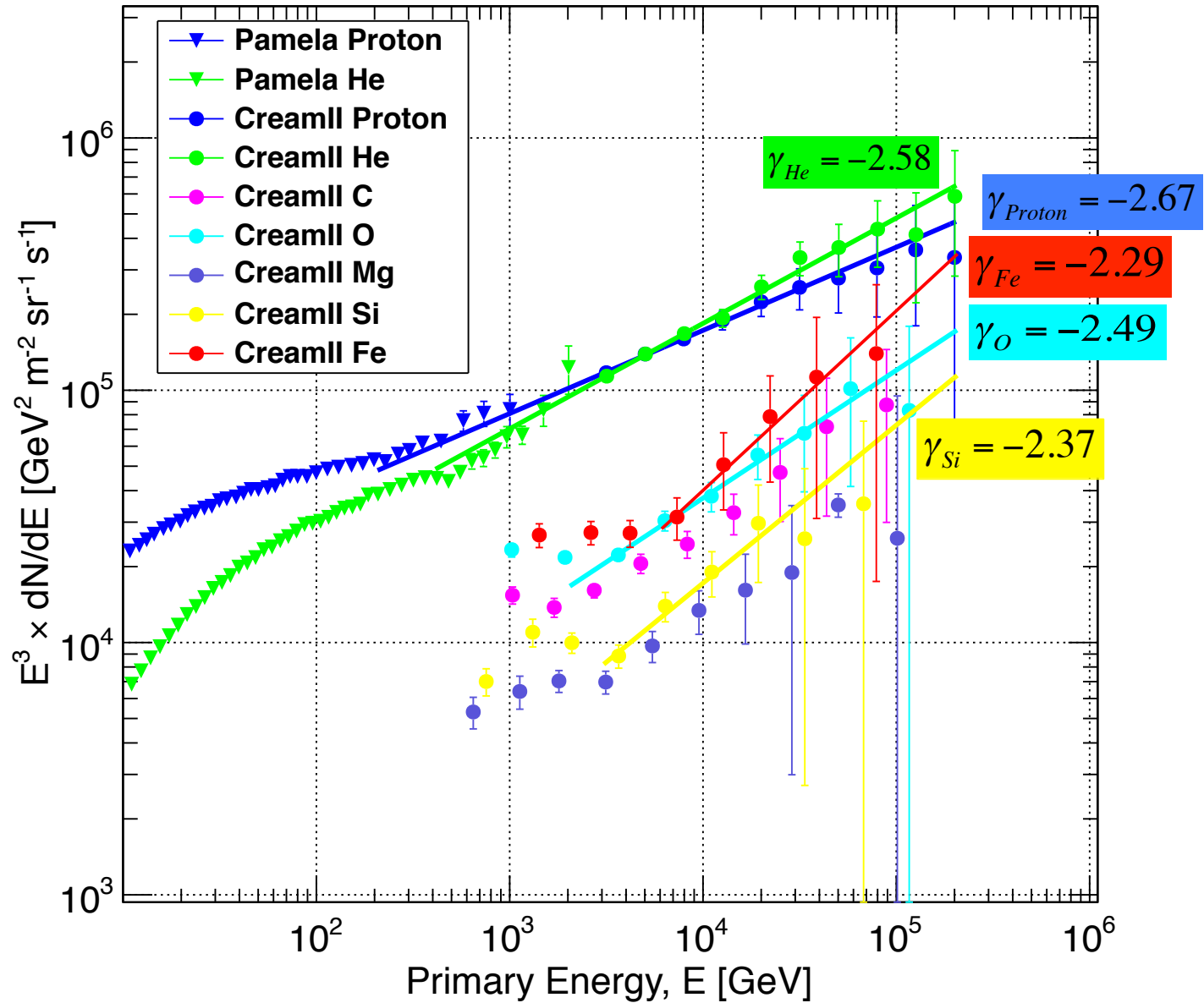
Perfect demonstration
 of Peters cycle:

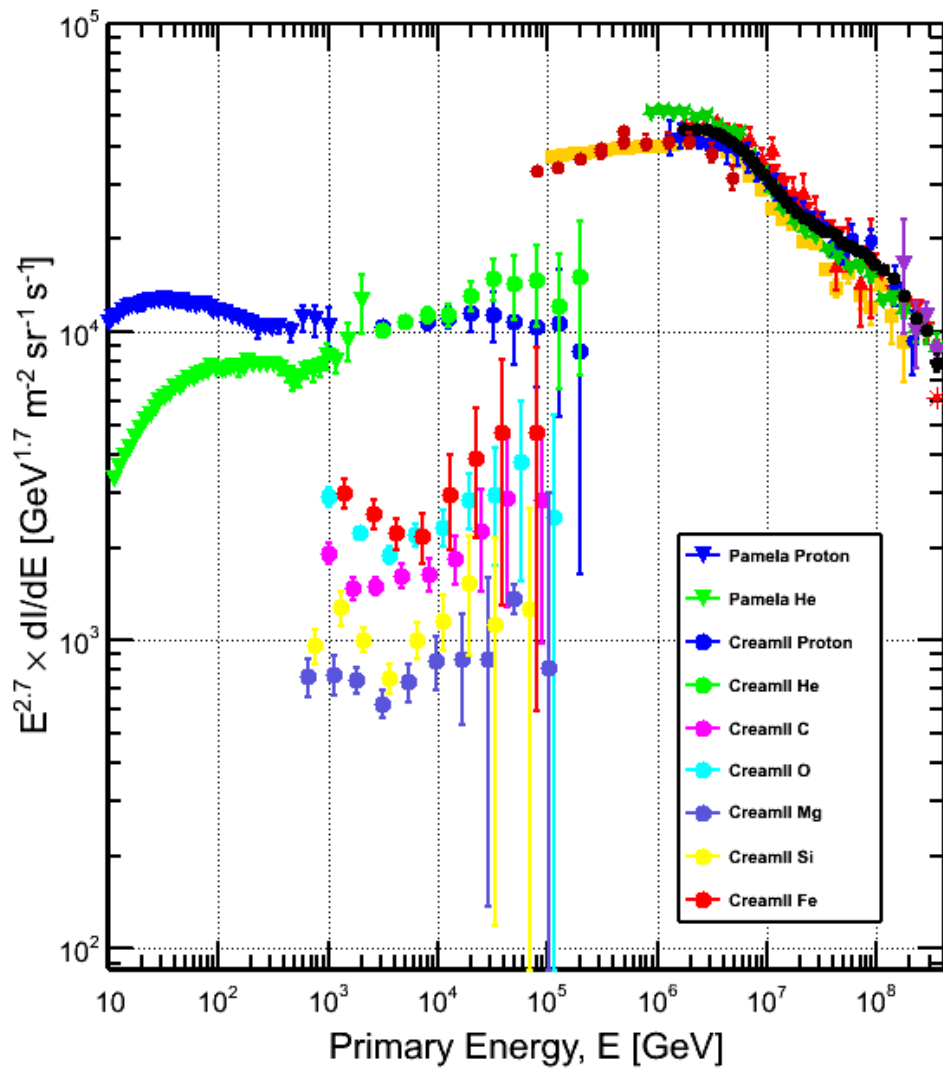
When protons accelerated
 to E_{max}^p a nucleus with Z will be
 accelerated up to
 $E_{max}^Z = Z \times R = Z \times E_{max}^p$

where magnetic rigidity
 $R = Pc/Z$

Bernard Peters 1961

Spectral Indices of the hard component



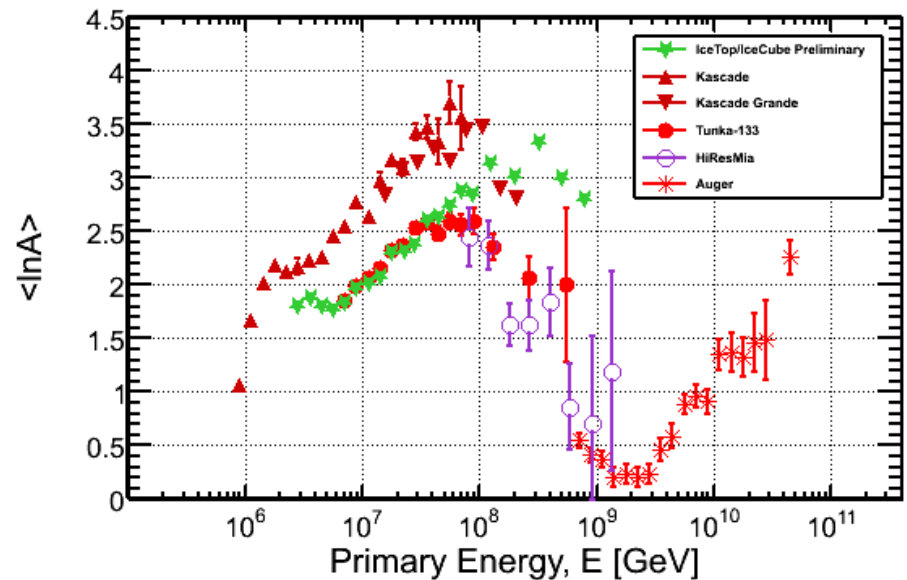


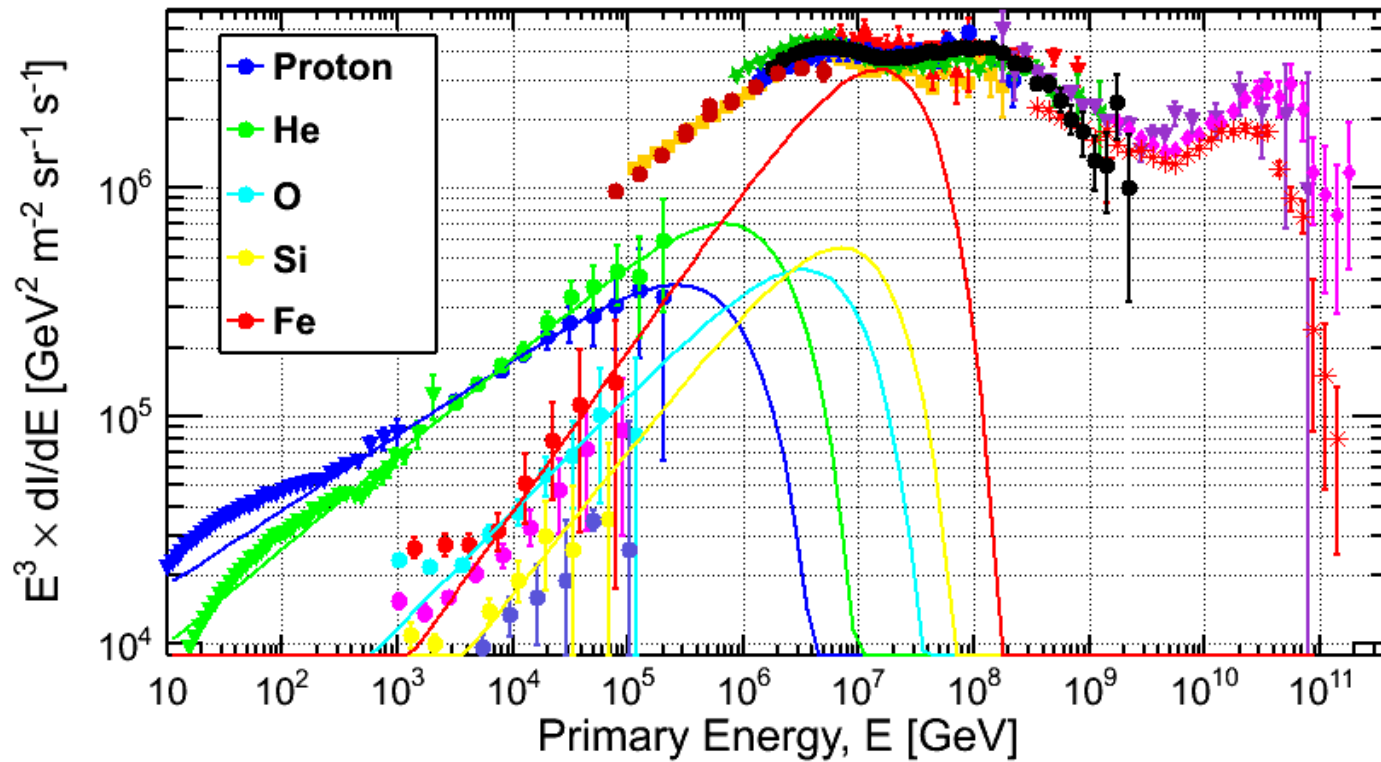
Fit the elemental spectrum with Gaisser's formulation of Peters cycle

$$E \frac{dN}{dE} = \sum_{\text{elements } i} A_i E^{-\gamma_i} e^{-\frac{E}{Z_i E_{\text{cutoff}}}}$$

A Amplitude
 γ spectral index
 E_{cutoff} cut-off energy

Above the knee use $\langle \ln A \rangle$ as guidance





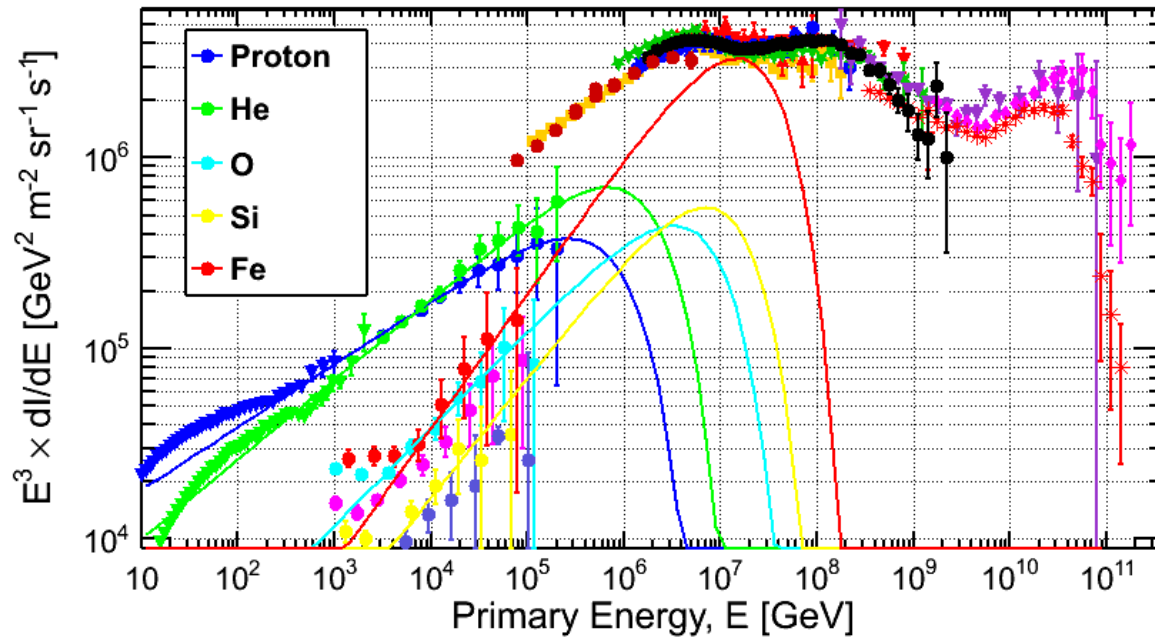
Amplitudes and indexes of all elements are defined by the CreamII data. Only the cutoffs need to be fit.

Fe spectrum is the key to the whole puzzle.

The Cream Fe data, when extended with the same index up to an energy where it makes 100% of the all particle spectrum, defines the maximum cut off energy for Fe.

This point turns out to be 20.8 PeV.

If Fe cuts off at 20.8 PeV → Proton will cut off at $20800/26 = 800$ TeV

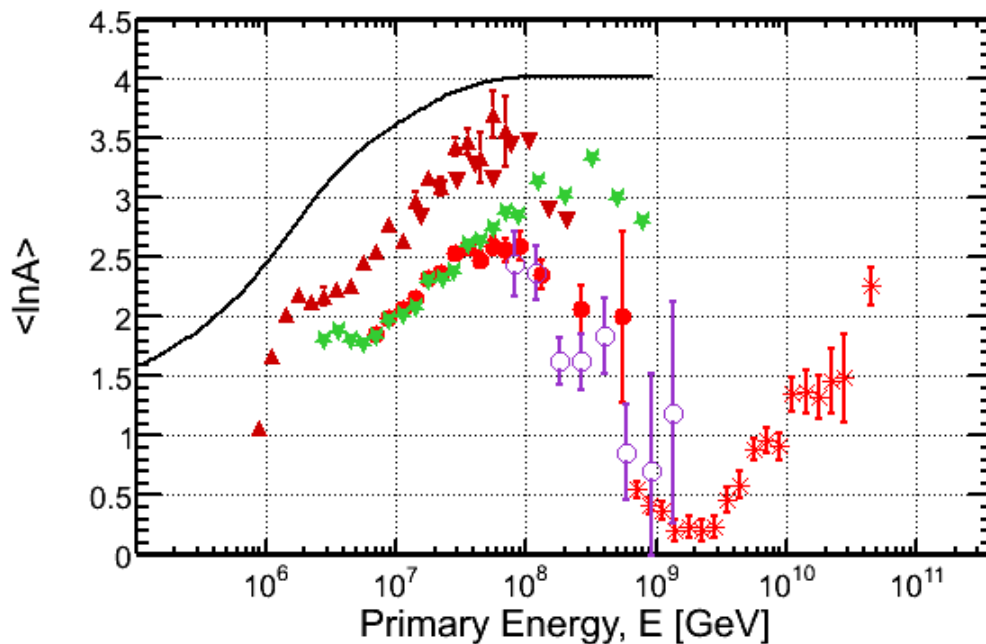


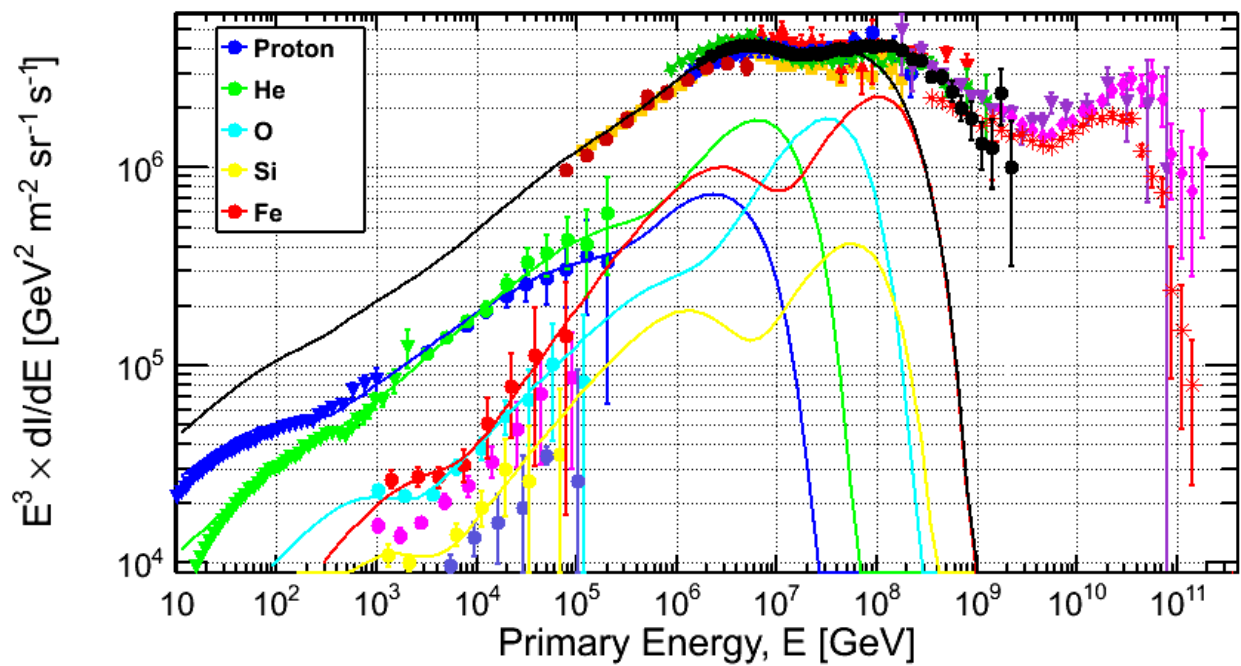
However

$\langle \ln A \rangle$ data tells us
the knee is not 100% Fe.

Since the amplitudes are locked
by the Cream data,
the only way to fit $\langle \ln A \rangle$ is
to bring the cutoff energy down

and fill the rest with elements
of a new Peters cycle
(a new population of particles)





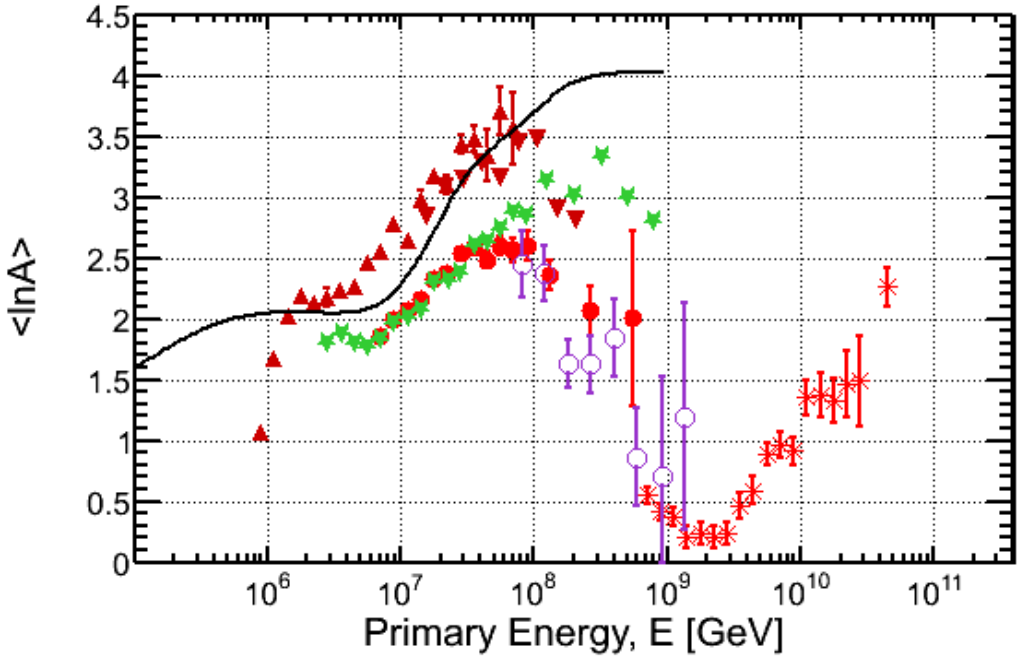
insert another Peter's cycle overlapping with the previous one until the best agreement with $\ln A$ is reached and constrained by the spectrum



$$90 \text{ TeV} < E^1_{cutoff} < 150 \text{ TeV}$$

and

$2 \text{ PeV} < E^2_{cutoff} < 4.5 \text{ PeV}$ with much harder spectral indices



$$\gamma_{Proton} = -2.3$$

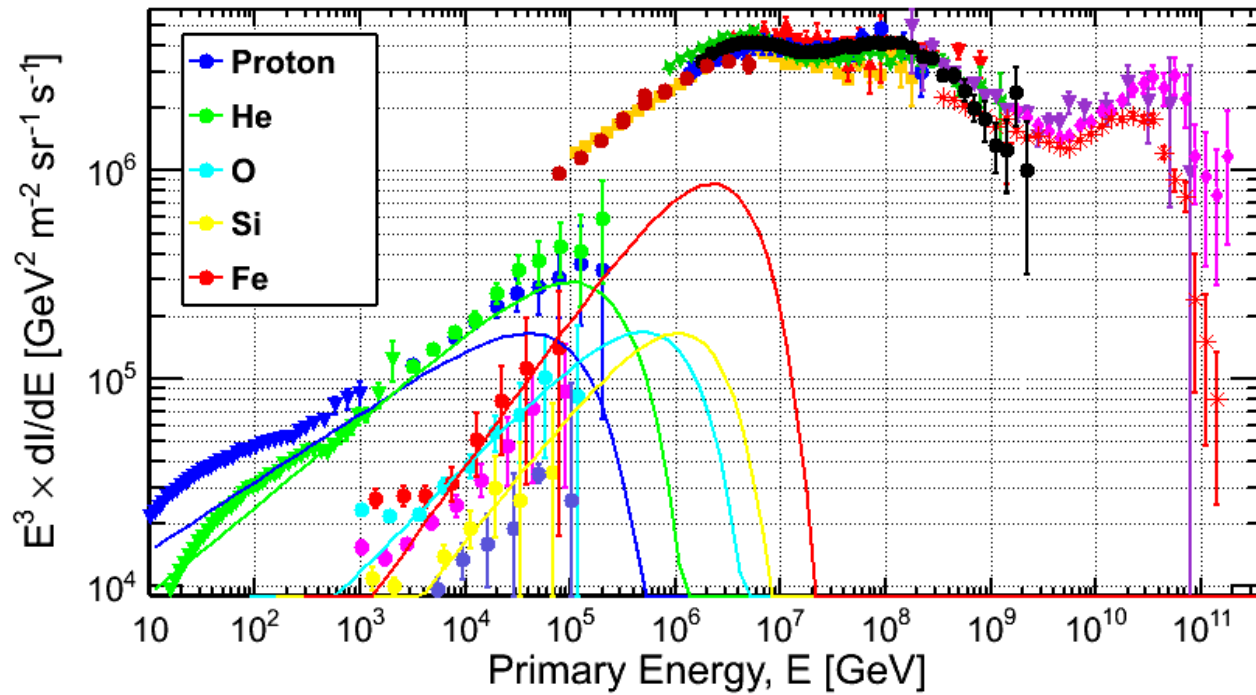
$$\gamma_{He} = -2.2$$

$$\gamma_{CNO} = -2.0$$

$$\gamma_{Si} = -2.0$$

$$\gamma_{Fe} = -2.0$$

The cosmic ray knee is the intersection of two different source populations



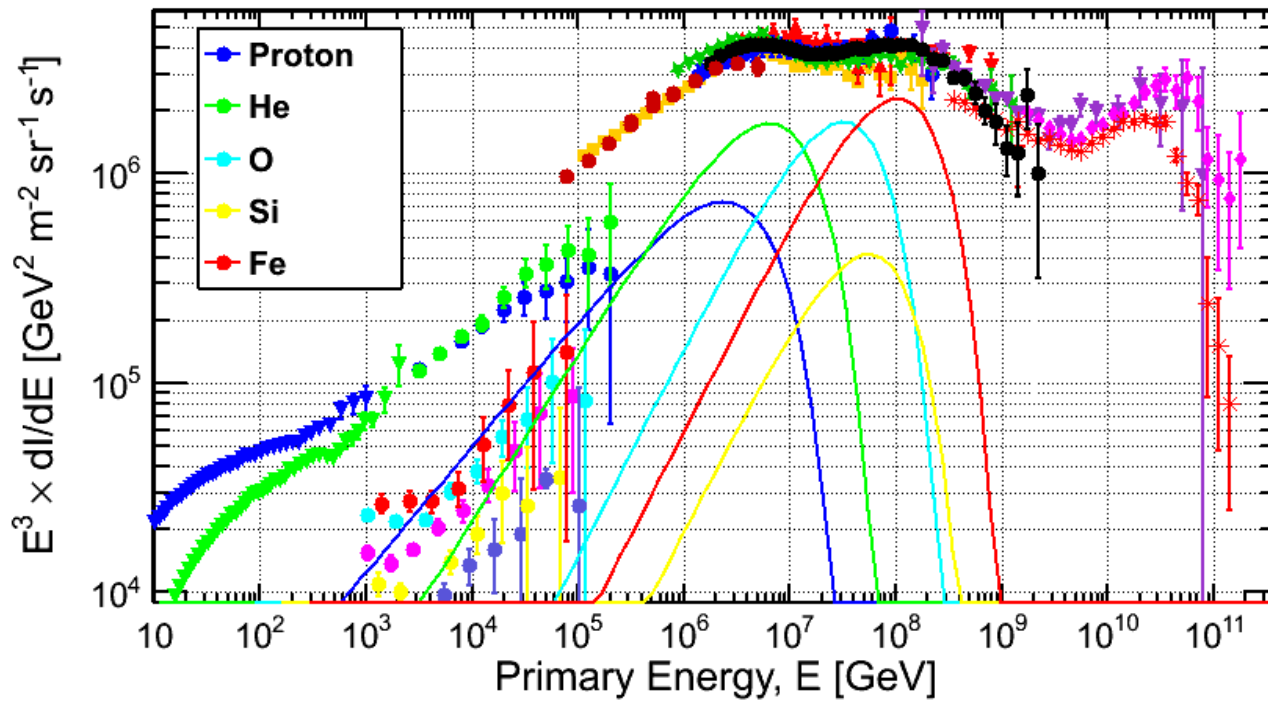
Cycle 1 alone

$$E_{cutoff}^P = 120 \text{ TeV}$$

$$E_{cutoff}^{Fe} = 26 \times 120 \text{ TeV} = 3.1 \text{ PeV}$$



The CR Knee



Cycle 2 alone

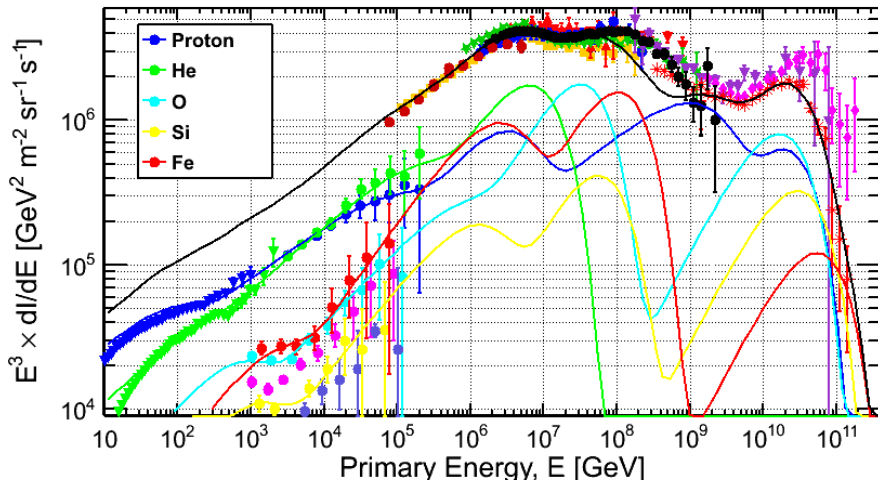
$$E_{cutoff}^P = 4 \text{ PeV}$$

$$E_{cutoff}^{Fe} = 26 \times 4 \text{ PeV} = 104 \text{ PeV}$$

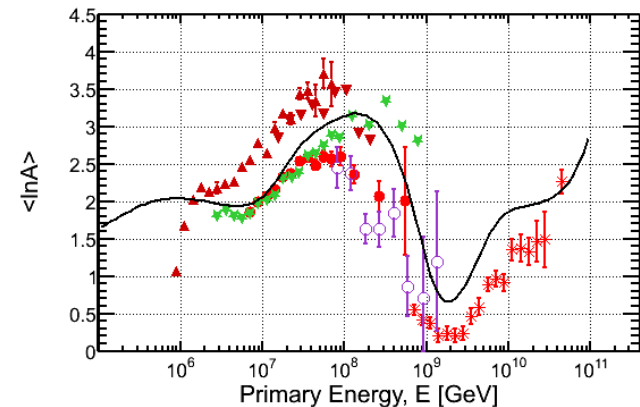
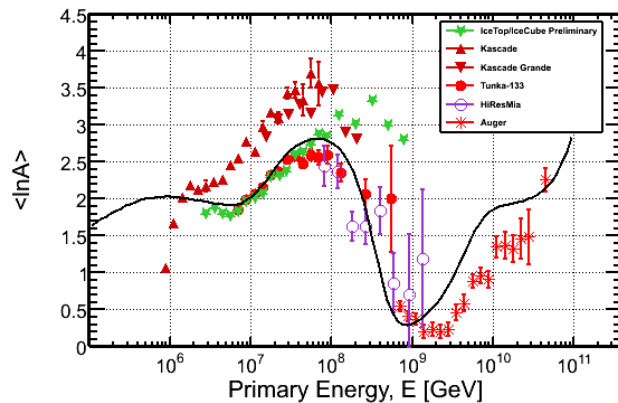
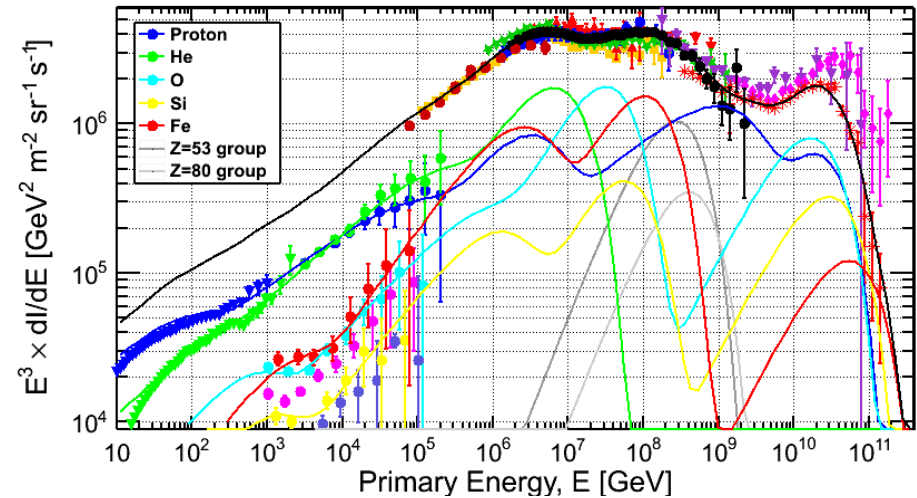
Proceed with the same method to inject another Peters cycle for UHE

- Try to fit Auger's composition as Cycle 3
- However, a gap is left between Cycle 2 and 3 and $\ln A$ turns to light too soon. There has to be some heavy elements at least upto 300 PeV.
 - ➔ include ultraheavy element groups as extension of Cycle 2 (as inspired by the lowE GCR measurements)

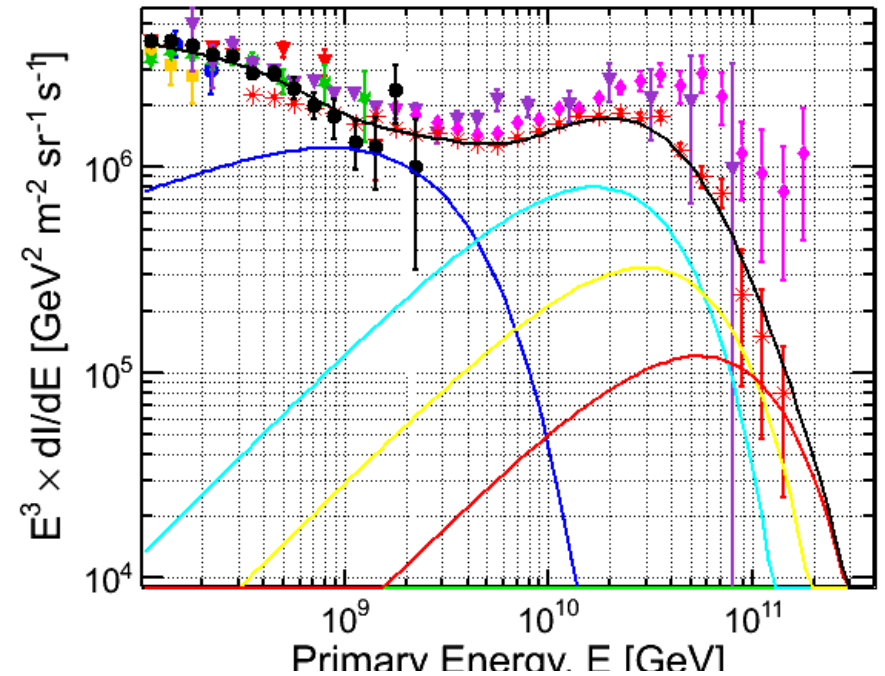
without ultraheavy nuclei



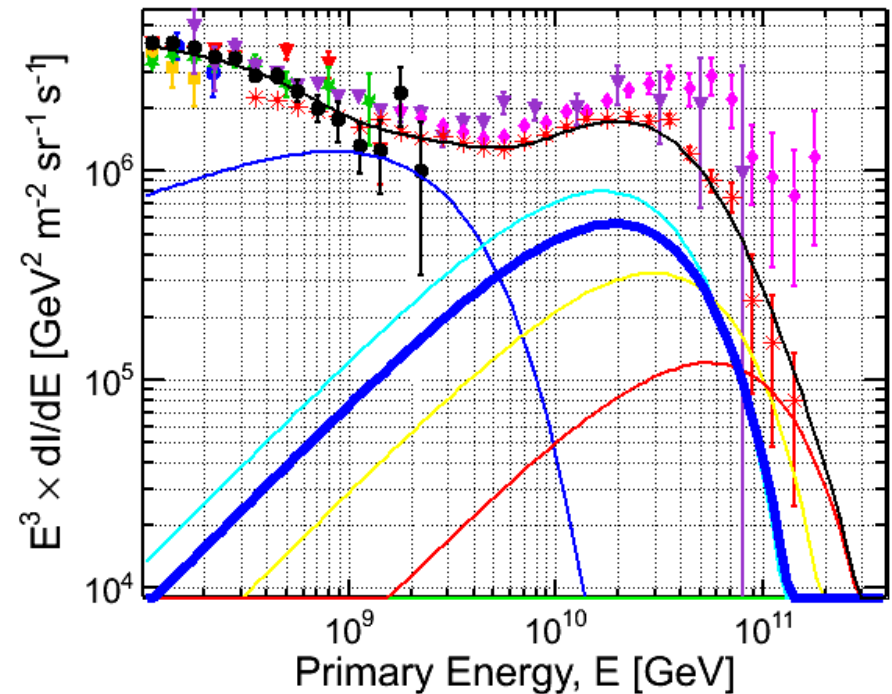
with ultraheavy nuclei



Auger fits to standard Peters cycle
 with Proton cut off at 2.1 EeV (index=2.6)
 No Helium could be accommodated
 Oxygen is dominant,
 but there has to be some Si and Fe as well



BUT: There is an EXTRA Proton
 which is not part of the standard cycle
 → this Proton cuts off ~ 20 EeV (index=2.0)



Compare with the Auger results: best performance is with EPOS-LHC

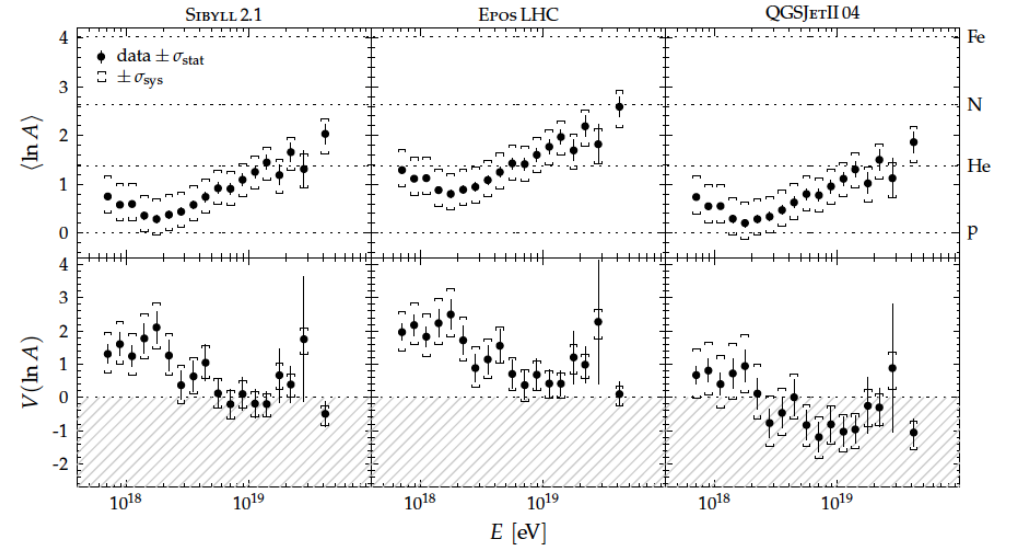
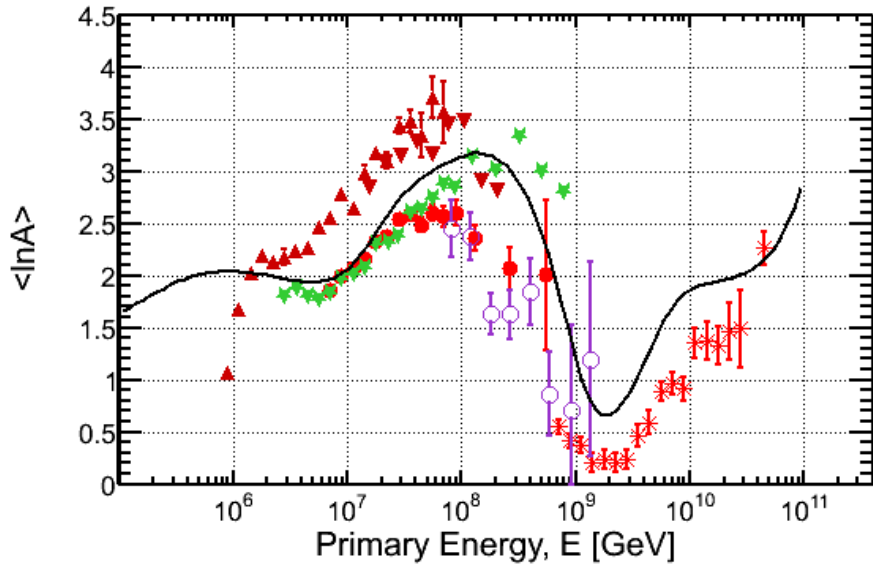


Figure 14: Average of the logarithmic mass and its variance estimated from data using different interaction models. The non-physical region of negative variance is indicated as the gray dashed region.

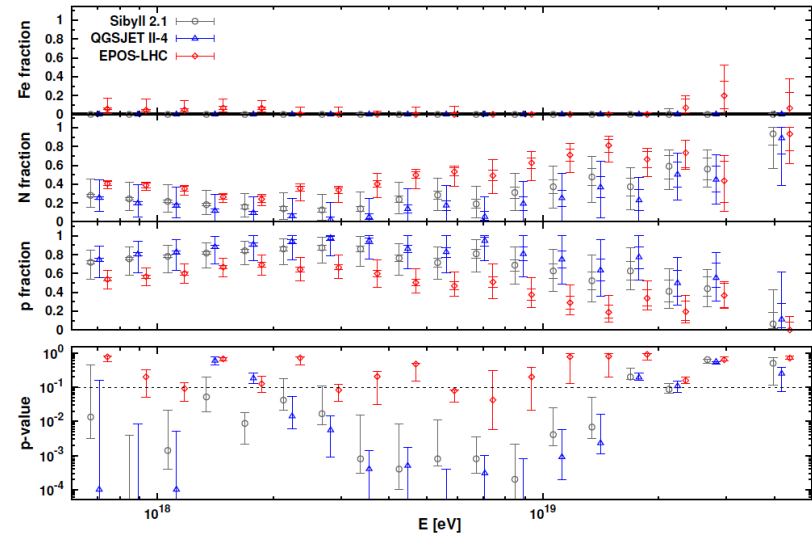
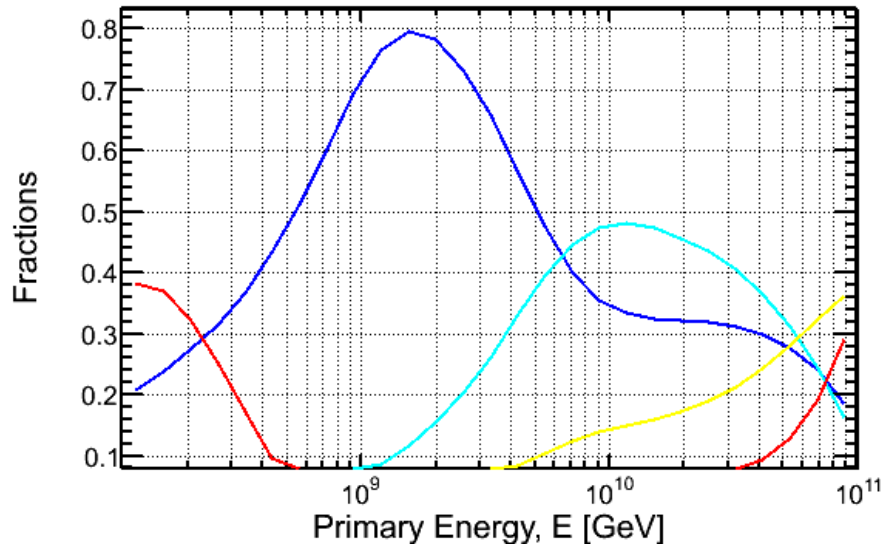
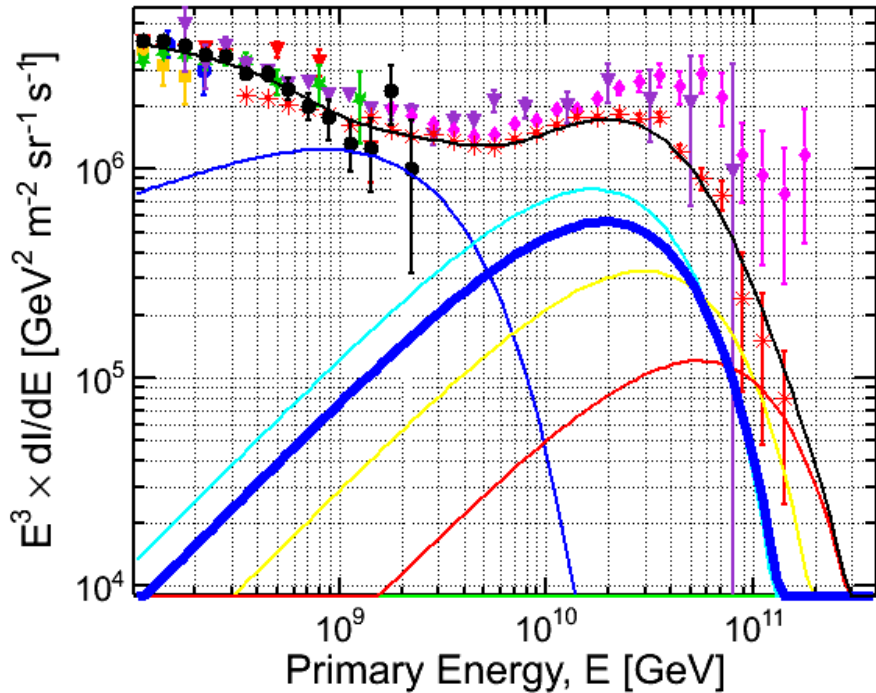
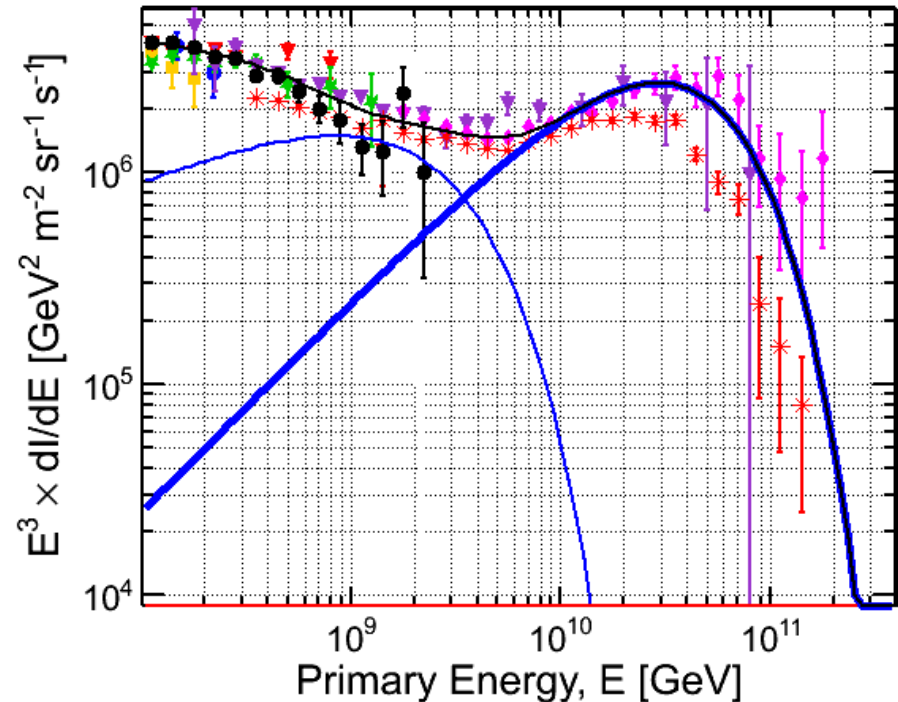


FIG. 3: Fitted fraction and quality for the scenario of a complex mixture of protons, nitrogen nuclei, and iron nuclei. The upper panels show the species fractions and the lower panel shows the p -values.

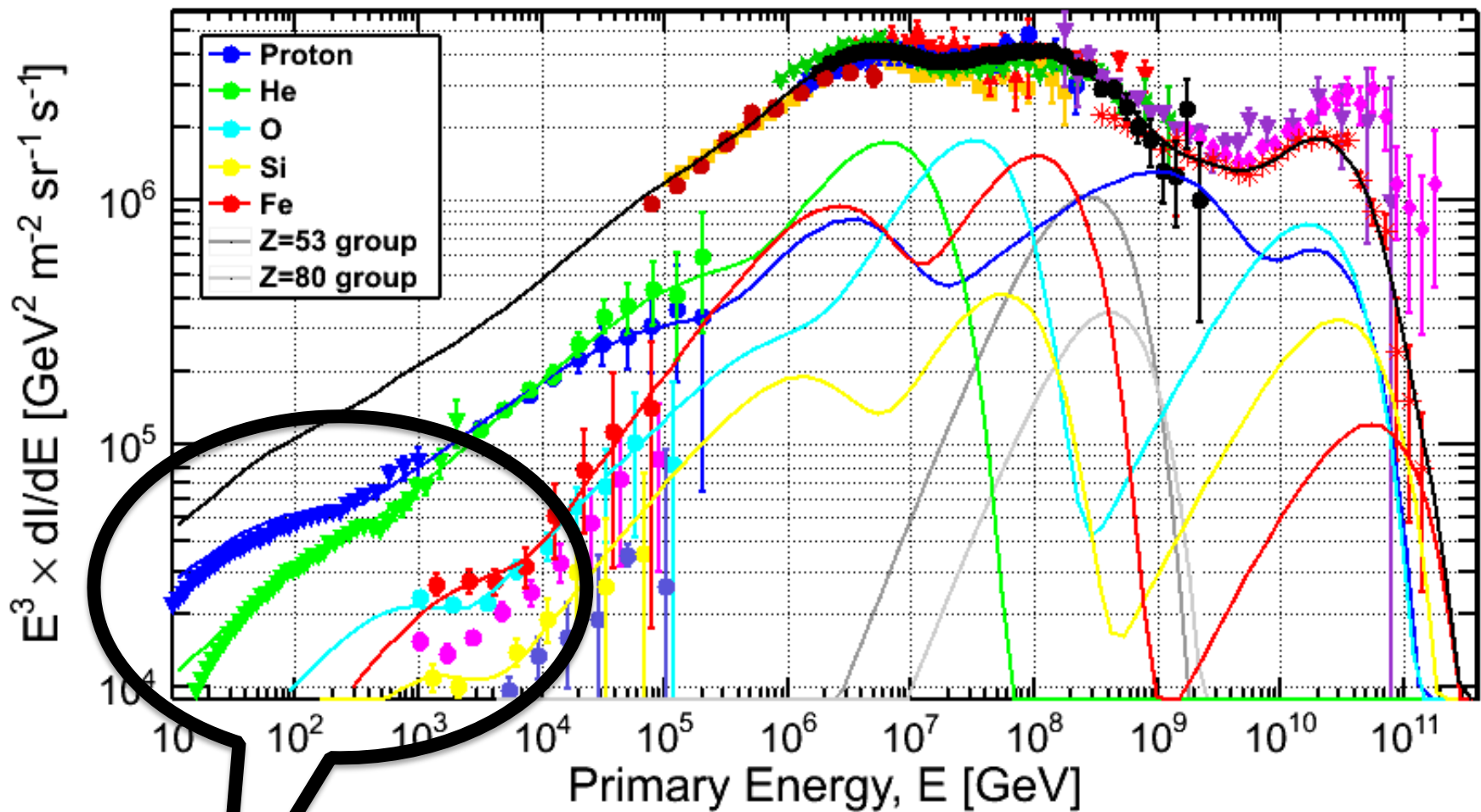
Compare Auger and TA



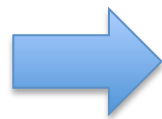
Auger sees heavy elements under extra-galactic Proton



TA sees all extra-galactic Proton (are the elements there in undetectable levels?)



There is yet another Peter's cycle here



A source population which cuts off around 100 GeV will explain the PAMELA break, which is the overlap between this population and the harder classic supernovae component setting in.

SNR IC443 "Jellyfish Nebula"
1.5 kpc away, ~10,000 yrs old



FERMI-LAT

SCIENCE VOL 339 15 FEBRUARY 2013

Detection of the Characteristic Pion-Decay Signature in Supernova Remnants

M. Ackermann,¹ M. Ajello,² A. Allafort,³ L. Baldini,⁴ J. Ballet,⁵ G. Barbiellini,^{6,7} M. G. Baring,⁸ D. Bastieri,^{9,10} K. Bechtol,³ R. Bellazzini,¹¹ R. D. Blandford,³ E. D. Bloom,³ E. Bonamente,^{12,13} A. W. Borgland,³ E. Bottacini,³ T. J. Brandt,¹⁴ J. Bregeon,¹¹ M. Brigida,^{15,16} P. Bruel,¹⁷ R. Buehler,³ G. Busetto,^{9,10} S. Buson,^{9,10} G. A. Caliendo,¹⁸ R. A. Cameron,³ P. A. Caraveo,¹⁹ J. M. Casandjian,⁵ C. Cecchi,^{12,13} Ö. Çelik,^{14,20,21} E. Charles,³ S. Chaty,⁵ R. C. G. Chaves,⁵ A. Chekhtman,²² C. C. Cheung,²³ J. Chiang,³ G. Chiaro,²⁴ A. N. Cillis,^{14,25} S. Ciprini,^{13,26} R. Claus,³ J. Cohen-Tanugi,²⁷ L. R. Cominsky,²⁸ J. Conrad,^{29,30,31} S. Corbel,^{5,32} S. Cutini,³³ F. D'Ammando,^{12,34,35} A. de Angelis,³⁶ F. de Palma,^{15,16} C. D. Dermer,³⁷ E. do Couto e Silva,³ P. S. Drell,³ A. Drlica-Wagner,³ L. Falletti,²⁷ C. Favuzzi,^{15,16} E. C. Ferrara,¹⁴ A. Franckowiak,³ Y. Fukazawa,³⁸ S. Funk,^{3*} P. Fusco,^{15,16} F. Gargano,¹⁶ S. Germani,^{12,13} N. Giglietto,^{15,16} P. Giommi,³³ F. Giordano,^{15,16} M. Giroletti,³⁹ T. Glanzman,³ G. Godfrey,³ I. A. Grenier,⁵ M.-H. Grondin,^{40,41} J. E. Grove,³⁷ S. Guiriec,¹⁴ D. Hadasch,¹⁸ Y. Hanabata,³⁸ A. K. Harding,¹⁴ M. Hayashida,^{3,42} K. Hayashi,³⁸ E. Hays,¹⁴ J. W. Hewitt,¹⁴ A. B. Hill,^{3,43} R. E. Hughes,⁴⁴ M. S. Jackson,^{30,45} T. Jogler,³ G. Jóhannesson,⁴⁶ A. S. Johnson,³ T. Kamae,³ J. Kataoka,⁴⁷ J. Katsuta,³ J. Knödlseher,^{48,49} M. Kuss,¹¹ J. Lande,³ S. Larsson,^{29,30,50} L. Latronico,⁵¹ M. Lemoine-Goumard,^{52,53} F. Longo,^{6,7} F. Loparco,^{15,16} M. N. Lovellette,³⁷ P. Lubrano,^{12,13} G. M. Madejski,³ F. Massaro,³ M. Mayer,¹ M. N. Mazziotta,¹⁶ J. E. McEnery,^{14,54} J. Mehault,²⁷ P. F. Michelson,³ R. P. Mignani,⁵⁵ W. Mitthumsiri,³ T. Mizuno,⁵⁶ A. A. Moiseev,^{20,54} M. E. Monzani,³ A. Morselli,⁵⁷ I. V. Moskalenko,³ S. Murgia,³ T. Nakamori,⁴⁷ R. Nemmen,¹⁴ E. Nuss,²⁷ M. Ohno,⁵⁸ T. Ohsugi,⁵⁶ N. Omodei,³ M. Orienti,³⁹ E. Orlando,³ J. F. Ormes,⁵⁹ D. Paneque,^{3,60} J. S. Perkins,^{14,21,20,61} M. Pesce-Rollins,¹¹ F. Piron,²⁷ G. Pivato,¹⁰ S. Rainò,^{15,16} R. Rando,^{9,10} M. Razzano,^{11,62} S. Razzaque,²² A. Reimer,^{3,63} O. Reimer,^{3,63} S. Ritz,⁶² C. Romoli,¹⁰ M. Sánchez-Conde,³ A. Schulz,¹ C. Sgrò,¹¹ P. E. Simeon,³ E. J. Siskind,⁶⁴ D. A. Smith,⁵² G. Spandre,¹¹ P. Spinelli,^{15,16} F. W. Stecker,^{14,65} A. W. Strong,⁶⁶ D. J. Suson,⁶⁷ H. Tajima,^{3,68} H. Takahashi,³⁸ T. Takahashi,⁵⁸ T. Tanaka,^{3,69*} J. G. Thayer,³ J. B. Thayer,³ D. J. Thompson,¹⁴ S. E. Thorsett,⁷⁰ L. Tibaldo,^{9,10} O. Tibolla,⁷¹ M. Tinivella,¹¹ E. Troja,^{14,72} Y. Uchiyama,^{3*} T. L. Usher,³ J. Vandenbroucke,³ V. Vasileiou,²⁷ G. Vianello,^{3,73} V. Vitale,^{57,74} A. P. Waite,³ M. Werner,⁶³ B. L. Winer,⁴⁴ K. S. Wood,³⁷ M. Wood,³ R. Yamazaki,⁷⁵ Z. Yang,^{29,30} S. Zimmer,^{29,30}

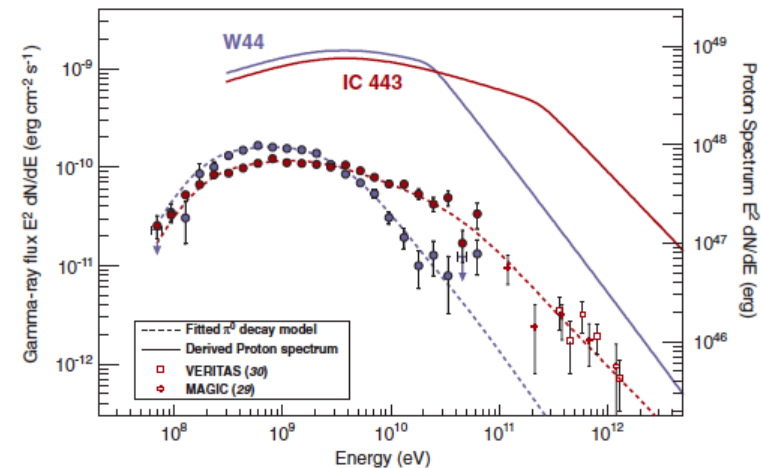
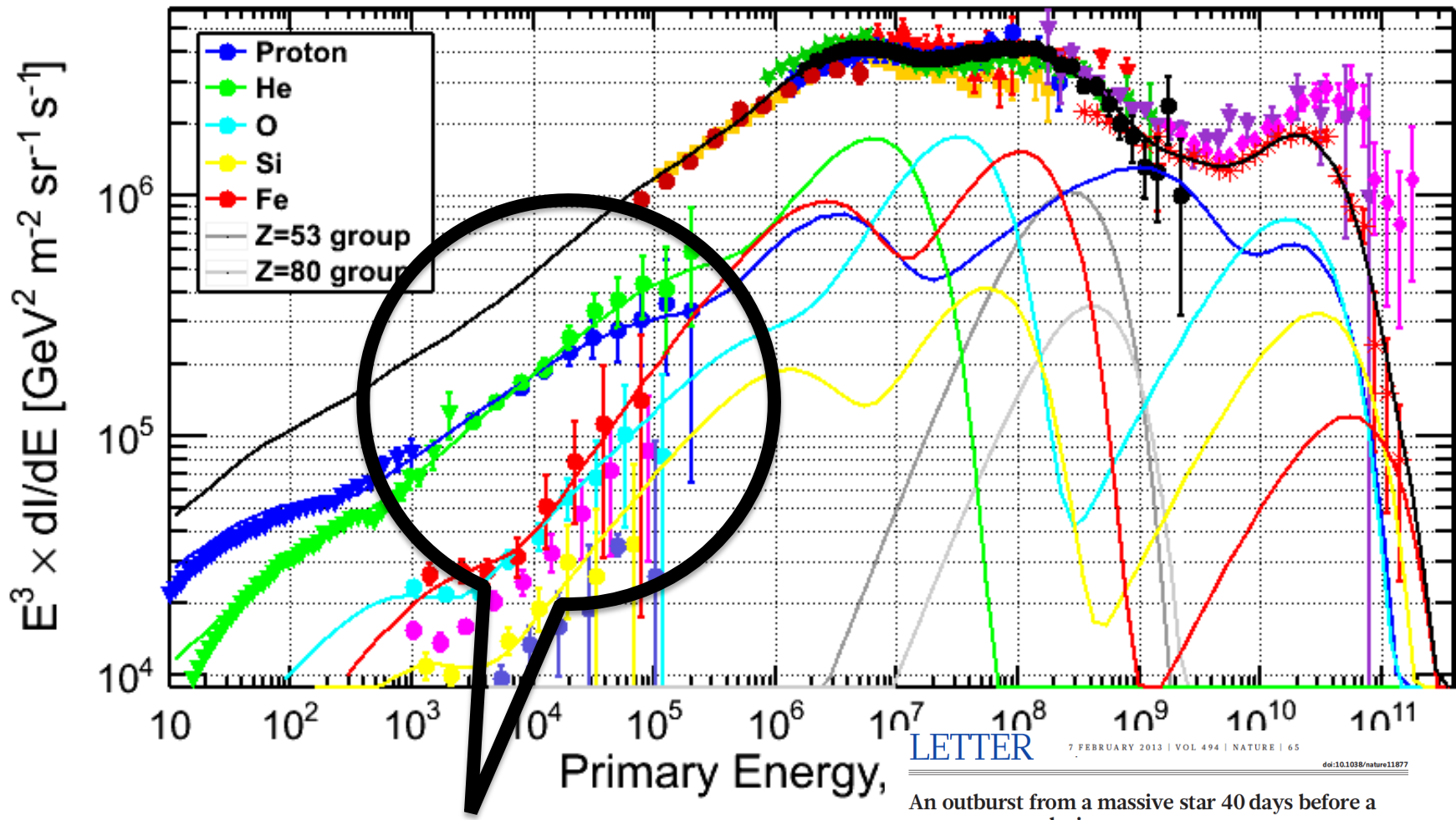


Fig. 3. Proton and gamma-ray spectra determined for IC 443 and W44. Also shown are the broadband spectral flux points derived in this study, along with TeV spectral data points for IC 443 from MAGIC (29) and VERITAS (30). The curvature evident in the proton distribution at ~2 GeV is a consequence of the display in energy space (rather than momentum space). Gamma-ray spectra from the protons were computed using the energy-dependent cross section parameterized by (32). We took into account accelerated nuclei (heavier than protons) as well as nuclei in the target gas by applying an enhancement factor of 1.85 (33). Note that models of the gamma-ray production via pp interactions have some uncertainty. Relative to the model adopted here, an alternative model of (6) predicts ~30% less photon flux near 70 MeV; the two models agree with each other to better than 15% above 200 MeV. The proton spectra assume average gas densities of $n = 20 \text{ cm}^{-3}$ (IC 443) and $n = 100 \text{ cm}^{-3}$ (W44) and distances of 1.5 kpc (IC 443) and 2.9 kpc (W44).



The classical supernovae cutting around 100 TeV

Massive stars, circumstellar ejecta

An outburst from a massive star 40 days before a supernova explosion

E. O. Ofek¹, M. Sullivan^{2,3}, S. B. Cenko⁴, M. M. Kasliwal¹, A. Gal-Yam¹, S. R. Kulkarni⁵, I. Arcavi¹, L. Bildsten^{6,8}, J. S. Bloom^{6,9}, A. Hoshino⁴, D. A. Howell¹⁰, A. V. Filippenko⁷, R. Laher¹¹, D. Murray¹², E. Nakar¹³, P. E. Nugent^{6,9}, J. M. Silverman^{1,14}, N. J. Shaviv¹⁵, J. Surace¹⁶ & O. Yaron¹

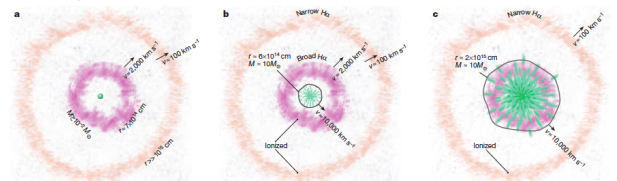
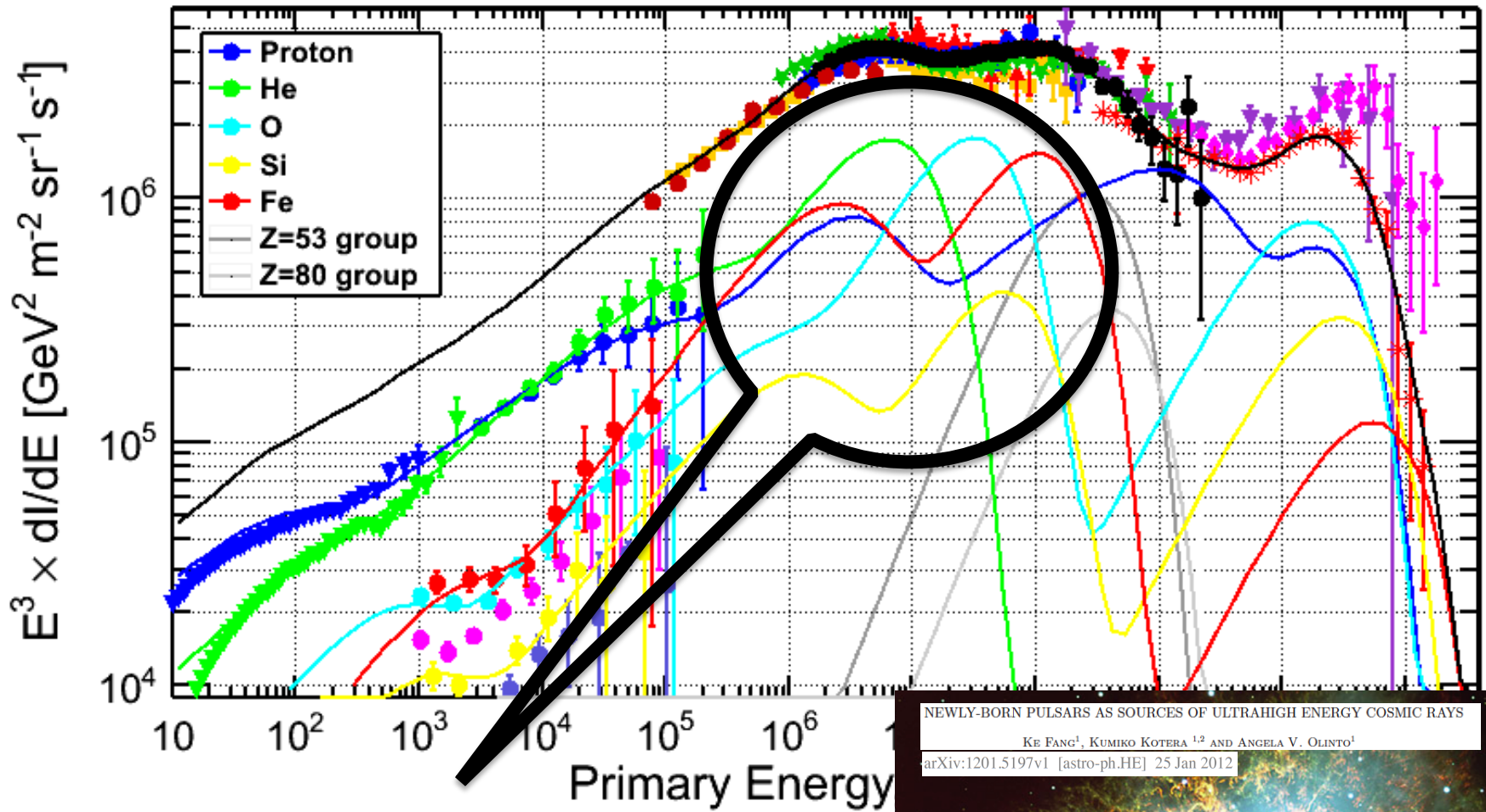


Figure 3 | Qualitative sketch of the proposed model for SN 2010bc. a, At day -40 (relative to the supernova explosion time), an inner shell (purple) with a mass of $\sim 10^{-2} M_{\odot}$, ejected about one month earlier during the precursor outburst and moving at velocity v of about $2,000 \text{ km s}^{-1}$, is located at a radius r of $\sim 7 \times 10^4 \text{ cm}$. An outer shell (orange), found at a larger radius and moving at about 100 km s^{-1} (up to 10^5 km s^{-1}), was ejected at earlier times. This indicates that the progenitor probably had multiple mass-loss episodes in the past tens to hundreds of years before the explosion. b, At day -5 , the supernova shock front (dark grey line) moving at $\sim 10,000 \text{ km s}^{-1}$ is ionizing the inner and outer shells which produce the broad and narrow H α emission seen in the early-time spectra. c, At day -20 , the supernova shock engulfs the inner shell, and the intermediate-width ($\sim 2,000 \text{ km s}^{-1}$) component of the H α line disappears. Instead we detect a $1,000 \text{ km s}^{-1}$ line, presumably due to material ejected during previous, but probably recent, mass-loss episodes and that is found at larger distances from the supernova. We note that inspection of the supernova light curve shows that around day 50 there is an indication of a possible rebrightening, perhaps resulting from the supernova ejecta colliding with such additional material ejected at earlier times. At day -20 , the photospheric temperature decreases and it becomes optically thinner, and therefore we begin seeing an H β Cygni profile with a velocity of $\sim 10,000 \text{ km s}^{-1}$. This line becomes even stronger on day 27. This reflects the unshocked ejecta below the interaction zone.



Fast spinning more massive stars
 beamed structure
 → Pulsar Wind Nebula systems

NEWLY-BORN PULSARS AS SOURCES OF ULTRAHIGH ENERGY COSMIC RAYS
 KE FANG¹, KUMIRO KOTERA^{1,2} AND ANGELA V. OLINTO¹
 arXiv:1201.5197v1 [astro-ph.HE] 25 Jan 2012

Newborn Pulsars
 as Sources of UHECRs

Ke Fang
 University of Chicago

KF, Kotera & Olinto, ApJ, 750:118, 2012

5

Cosmic Ray Anisotropy Workshop
 Sep 26 2013

Observation of High-Energy Astrophysical Neutrinos in Three Years of IceCube Data

arXiv:1405.5303v2 [astro-ph.HE] 2 Jul 2014

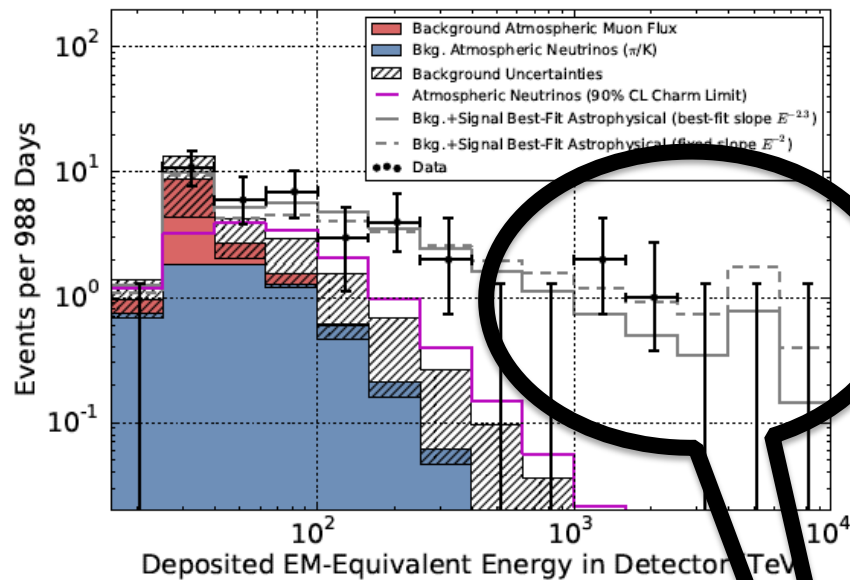


FIG. 2. Deposited energies of observed events with predictions. The hashed region shows uncertainties on the sum of all backgrounds. Muons (red) are computed from simulation to overcome statistical limitations in our background measurement and scaled to match the total measured background rate. Atmospheric neutrinos and uncertainties thereon are derived from previous measurements of both the π/K and charm components of the atmospheric ν_μ spectrum [9]. A gap larger than the one between 400 and 1000 TeV appears in 43% of realizations of the best-fit continuous spectrum.

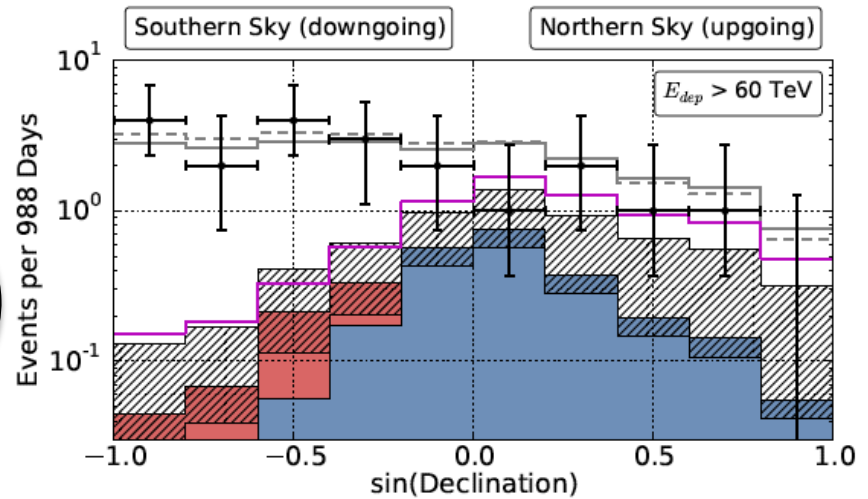


FIG. 3. Arrival angles of events with $E_{dep} > 60$ TeV, as used in our fit and above the majority of the cosmic ray muon background. The increasing opacity of the Earth to high energy neutrinos is visible at the right of the plot. Vetoing atmospheric neutrinos by muons from their parent air showers depresses the atmospheric neutrino background on the left. The data are described well by the expected backgrounds and a hard astrophysical isotropic neutrino flux (gray lines). Colors as in Fig. 2. Variations of this figure with other energy thresholds are in the online supplement [29].

1-2 PeV neutrinos as secondaries will come from ~ 20 -40 PeV region of CR spectrum

6 source populations explain the observed CR spectrum and $\langle \ln A \rangle$

Source 1: The Sun (cutting off around 10 GeV)

Population 2: Old SNR (~10-20 kyrs old, e.g. IC443, W44, W28), cuts off ~100GeV

Population 3: The classical supernova cutting off around 100 TeV, ~1-3 in 100 yrs

Massive stars, circumstellar ejecta

Population 4: “Galactic PeVatron”: PWN/Hypernovae, 1 in 1000 yrs → TeV –PeV neutrinos

Fast spinning massive stars with mass 20-50 M_{sun} , beamed structure

found in star forming regions, live wild, die young,

leave a fast spinning pulsar behind

Population 5: “Galactic EeVatron”: Hypernovae/GRB, 1 in 10000 yrs → PeV neutrinos

Population 6: extragalactic Proton: superposed on population 5 → PeV neutrinos

IceCube’s TeV-PeV neutrinos are a mixture of Pop4 + Pop5 + Pop6 (galactic + extragalactic)